City of Morro Bay and
Cayucos Sanitary District

OFFSHORE MONITORING AND REPORTING PROGRAM

SECOND QUARTER RECEIVING–WATER SURVEY

MAY 2017

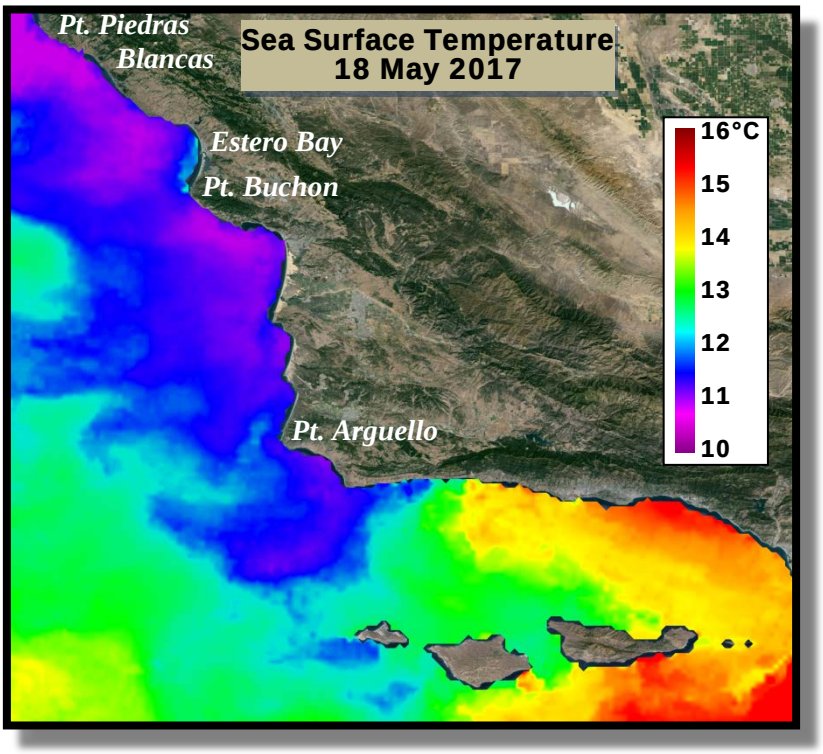

Marine Research Specialists
4744 Telephone Rd Ste 3 PMB 315
Ventura, California 93003

Report to the

City of Morro Bay and
Cayucos Sanitary District

955 Shasta Avenue
Morro Bay, California 93442
(805) 772-6272

OFFSHORE MONITORING AND REPORTING PROGRAM

SECOND QUARTER RECEIVING–WATER SURVEY

MAY 2017

Prepared by

Douglas A. Coats

Marine Research Specialists

4744 Telephone Rd Ste 3 PMB 315
Ventura, California 93003

Telephone: (805) 644-1180
E-mail: Marine@Rain.org

July 2017

marine research specialists
4744 Telephone Rd., STE 3 PMB 315 • Ventura, CA 93003 • 805-644-1180

John Gunderlock
Wastewater & Collection Systems Supervisor
City of Morro Bay
955 Shasta Avenue
Morro Bay, CA 93442

11 July 2017

Reference: Second Quarter Receiving-Water Survey Report – May 2017

Dear Mr. Gunderlock:

The attached report presents results from a quarterly receiving-water survey conducted on Thursday, 25 May 2017. The survey was conducted in accordance with the requirements of the NPDES permit issued to the City and District for discharge of treated wastewater to Estero Bay. The report evaluated compliance with permit limitations and assessed the effectiveness of effluent dispersion within receiving waters. Quantitative analyses of continuous instrumental measurements and qualitative visual observations confirmed that the wastewater discharge complied with the receiving-water limitations specified in the permit, and with the objectives of the California Ocean Plan.

The offshore measurements confirmed that the diffuser structure and treatment plant continued to operate at a high level of performance. The measurements delineated a diffuse discharge plume containing low organic loads within a highly localized region north of the discharge point. Dilution within the plume exceeded expectations based on modeling and outfall design criteria.

Contact the undersigned if you have questions regarding the attached report.

Sincerely,

Douglas A. Coats

Douglas A. Coats
Program Manager

I certify under penalty of law that this document and all attachments were prepared under my direction or supervision in accordance with a system designed to assure that qualified personnel properly gather and evaluate the information submitted. Based on my inquiry of the person or persons who manage the system, or those persons directly responsible for gathering the information, the information submitted is, to the best of my knowledge and belief, true, accurate and complete. I am aware that there are significant penalties for submitting false information, including the possibility of fine and imprisonment for knowing violations.

Mr. John Gunderlock
Wastewater/Collections System Supervisor
City of Morro Bay/Cayucos CSD Wastewater Treatment Plant

Date: 7/11/17

TABLE OF CONTENTS

LIST OF FIGURES

LIST OF TABLES

INTRODUCTION

The City of Morro Bay and the Cayucos Sanitary District (MBCSD) jointly own the wastewater treatment plant (WWTP) operated by the City of Morro Bay. In March 1985, Region IX of the U.S. Environmental Protection Agency (USEPA) and the Central Coast California Regional Water Quality Control Board (RWQCB) issued the first National Pollutant Discharge Elimination System (NPDES) permit to the MBCSD. The permit incorporated partially modified secondary treatment requirements for the plant's ocean discharge. The permit has been re-issued three times, in March 1993 (RWQCB-USEPA 1993ab), December 1998 (RWQCB-USEPA 1998ab), and January 2009 (RWQCB-USEPA 2009). The May 2017 field survey described in this report was the thirty-fourth receiving-water survey conducted under the current permit.

The NPDES discharge permit requires seasonal monitoring of offshore receiving-water quality with quarterly surveys. This report summarizes the results of sampling conducted on 25 May 2017. Specifically, this second-quarter survey captured ambient oceanographic conditions along the central California coast during the spring season. The survey's measurements were used to assess the discharge's compliance with the objectives of the California Ocean Plan (COP) and the Central Coast Basin Plan (RWQCB 1994) as promulgated by the receiving-water limitations specified in the NPDES discharge permit.

The monitoring objectives were achieved by empirically evaluating tabulations of instrumental measurements and standard field observations. In addition to the traditional, vertical water-column profiles, instrumental measurements were used to generate horizontal maps from high-resolution data gathered by towing a CTD[1] instrument package repeatedly over the diffuser structure. This allowed for a more precise delineation of the plume's lateral extent.

SURVEY SETTING

The MBCSD treatment plant is located within the City of Morro Bay, which is situated along the central coast of California halfway between Los Angeles and San Francisco. Effluent is carried from the onshore treatment plant through a 1,450-m long outfall pipe, which terminates at a diffuser structure on the seafloor 827 m from the shoreline within Estero Bay (Figure 1). The diffuser structure extends an additional 52 m toward the northwest from the outfall terminus and consists of 34 ports that are hydraulically designed to create a turbulent ejection jet that rapidly mixes effluent with receiving seawater upon discharge. Currently, six of the diffuser ports are closed, thereby improving effluent dispersion by increasing the ejection velocity from the remaining 28 ports distributed along a 42-m section of the diffuser structure.

Following discharge from the diffuser ports, additional turbulent mixing occurs as the buoyant plume of dilute effluent ascends through the water column. Most of this buoyancy-induced mixing occurs within a zone of initial dilution (ZID), whose lateral reach in modeling studies extends 15.2 m from the centerline of the diffuser structure. Beyond the ZID, energetic waves, tides, and coastal currents within Estero Bay further disperse the dilute effluent within the open-ocean receiving waters. Both vertical hydrocasts and horizontal tow surveys are conducted around the diffuser structure to assess the efficacy of the diffuser, to define the lateral extent of the discharge plume, and to evaluate compliance with the NPDES permit limitations.

[1] Conductivity, temperature, and depth (CTD)

Figure 1. Location of the Receiving-Water Survey Area

Near the diffuser, prevailing flow generally follows bathymetric contours that parallel the north-south trend of the adjacent coastline. Because of the rapid initial mixing achieved within 15 m of the diffuser structure, impingement of unmixed effluent onto the adjacent coastline, 827 m away, is highly unlikely. Nevertheless, in the event of a failure in the treatment plant's disinfection system, collection and analysis of water samples at the eight surfzone-sampling stations shown in Figure 1 would be conducted to monitor for potential shoreline impacts. These surfzone samples would be analyzed for total and fecal coliform, and enterococcus bacterial densities.

Areas of special concern, such as the Morro Bay National Estuary and the Monterey Bay National Marine Sanctuary, are not affected by the discharge because they are even more distant from the outfall location. For example, the southern boundary of the Monterey Bay National Marine Sanctuary is located 38 km to the north, while the entrance to the Morro Bay National Estuary lies 2.8 km south. The southerly orientation of the mouth of the Bay, and the presence of Morro Rock 2 km to the south, serve to further limit direct seawater exchange between the discharge point and the Bay (Figure 1).

SAMPLING LOCATIONS

As shown in Figure 2, the offshore sampling pattern consists of six fixed offshore stations located within 100 m of the outfall diffuser structure. The red ⊙ symbols in the Figure indicate the target locations of the sampling stations (Table 1). The stations are situated at three distances relative to the center of the diffuser structure, and lie along a north-south axis at the same water depth (15.2 m) as the center of the diffuser. Depending on the direction of the local oceanic currents at the time of sampling, the discharge may influence one or more of these stations. The up-current stations on the opposite side of the diffuser then act as reference stations. Comparisons between the water properties at these antipodal stations quantify departures from ambient seawater properties caused by the discharge and allow compliance with the NPDES discharge permit to be determined.

The finite size of the diffuser is an important consideration in the assessment of wastewater dispersion close to the discharge. Although the discharge is considered a "*point source*" for modeling and regulatory purposes, it does not occur at a single isolated point of infinitesimal size. Instead, the discharge is distributed along a 42 m section of the seafloor, and, ultimately, the amount of wastewater dispersion at a given point in the water column is dictated by its distance from the closest diffuser port, rather than its distance from the center of the diffuser structure. This "*closest approach*" distance can be considerably less than the centerpoint distance normally cited in modeling studies (compare the last two columns of Table 1).

Another important consideration for compliance evaluation is the ability to determine the actual location of the measurements. Discerning small spatial separations within the compact sampling pattern only became feasible after the advent of Differential Global Positioning Systems (DGPS). The accuracy of traditional navigation systems such as LORAN or standard GPS is typically ±15 m, a span equal to half the total width of the ZID itself. DGPS incorporates a second signal from a fixed, land-based beacon that continuously transmits position errors in standard GPS readings to the DGPS receiver aboard the survey vessel. Real-time correction for these position errors provides an extremely stable and accurate offshore navigational reading with position errors of no more than 2 m, and often with sub-meter accuracy.

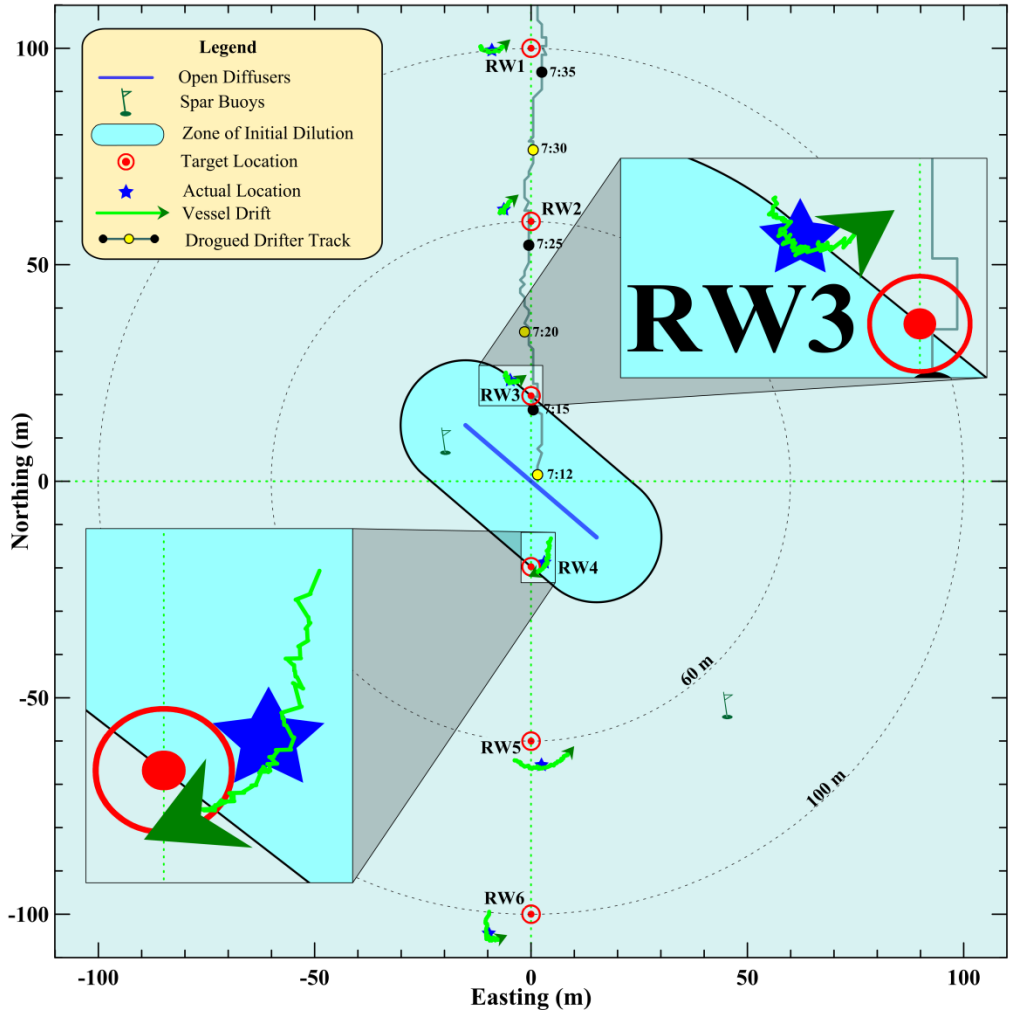

Figure 2. Station Locations

Table 1. Target Locations of the Receiving-Water Monitoring Stations

Station	Description	Latitude	Longitude	Center Distance[2] (m)	Closest Approach Distance[3] (m)
RW1	Upcoast Midfield	35° 23.253' N	120° 52.504' W	100	88.4
RW2	Upcoast Nearfield	35° 23.231' N	120° 52.504' W	60	49.4
RW3	Upcoast ZID	35° 23.210' N	120° 52.504' W	20	15.0
RW4	Downcoast ZID	35° 23.188' N	120° 52.504' W	20	15.0
RW5	Downcoast Nearfield	35° 23.167' N	120° 52.504' W	60	49.4
RW6	Downcoast Midfield	35° 23.145' N	120° 52.504' W	100	88.4

[2] Distance to the center of the open diffuser section
[3] Distance to the closest open diffuser port

During a diver survey in July 1998, the survey vessel's new DGPS navigation system, consisting of a Furuno™ GPS 30 and FBX2 differential beacon receiver, was used to precisely determine the position of the open section of the diffuser structure (MRS 1998) and establish the target locations for the receiving-water monitoring stations shown in Figure 2 and listed in Table 1. Presently, the use of two independent DGPS receivers aboard the survey vessel allows access to two separate land-based beacons for navigational intercomparison, ensuring extremely accurate and uninterrupted navigational reports.

Recording of DGPS positions at one-second intervals allows precise determination of sampling locations throughout the vertical CTD profiling conducted at the six individual stations, as well as during the tow survey. Knowledge of the precise location of individual CTD measurements relative to the diffuser is critical for accurate interpretation of the water-property fields. During vertical-profile sampling, the actual measurement locations rarely coincide with the target coordinates listed in Table 1 because winds, waves, and currents induce unavoidable horizontal offsets (drift). Even during quiescent metocean[4] conditions, the residual momentum of the survey vessel as it approaches the target locations can create perceptible offsets. Using DGPS however, these offsets can be quantified, and the vessel location can be precisely tracked throughout sampling at each station.

The May 2017 hydrocasts were conducted progressing from north to south, beginning with Station RW1. The magnitude of the drift at each of the six stations during the May 2017 survey is apparent from the length of the green tracklines in Figure 2. The tracklines trace the horizontal movement of the CTD as it was lowered to the seafloor at each station. Their lengths and offsets from the target locations reflect the overall station-keeping ability during the May 2017 survey.

The time it took the CTD to traverse the water column to the seafloor, which averaged 1 min 13 s, was consistent among stations, while the lateral distance traversed by the instrument package varied considerably among the stations, as did the direction of the drift (Figure 2). The lateral distance traversed by the instrument package during the downcasts was less than 4 m at Stations RW2 and RW3, but at Station RW5, the CTD moved more than 12 m during the downcast. The lateral movement of the CTD at any given time is determined by a complex interplay between the external influences of winds and currents, and the vessel's residual momentum immediately prior to each downcast. For example, the increased eastward drift at Station RW5 arose from the vessel's greater residual momentum as it approached the station from the west. The vessel slowly approached most other stations from the north and a light onshore breeze transported the vessel slowly toward the east during downcasts.[5] Additionally, the strong northward current flow, reflected in the drogued-drifter trajectory in Figure 2,[6] introduced a northeastward curvature in the CTD movement as it approached the seafloor at most stations.

Regardless of the cause, detailed knowledge of the CTD's movement during downcasts is important for the interpretation of the water-quality measurements. Because the target locations for Stations RW3 and RW4 lie along the ZID boundary (viz., the red ⊙ symbols in the insets in Figure 2), knowledge of the CTD's location during the downcasts at those stations is especially important in the compliance evaluation. This is because the receiving-water limitations specified in the COP only apply to measurements recorded along or beyond the ZID boundary, where initial mixing is assumed complete.

[4] Meteorological and oceanographic conditions include winds, waves, tides, and currents.
[5] Refer to Table 4 later in this report.
[6] Refer to the partial drogued drifter track shown in Figure 2 and the full track in Figure 3 later in this report.

During the May 2017 survey, only a small portion[7] of the data collected at Station RW4 was subject to the compliance assessment because the CTD remained well within the ZID throughout most of the downcast. The CTD only traversed the ZID boundary as it approached the seafloor during its transport toward the southwest.[8] Thus, only the data recorded within 1 m of the seafloor at Station RW4 were subject to the compliance analysis. Similarly, only some of the data collected at Station RW3 were subject to a compliance assessment because the CTD traveled along the ZID boundary during the downcast, and only moved beyond the boundary at the beginning and end of the cast (upper right inset in Figure 2).

Compliance assessments notwithstanding, measurements acquired within the ZID lend valuable insight into the outfall's effectiveness at dispersing wastewater. For example, low dilution rates and concentrated effluent throughout the ZID would indicate potentially damaged or broken diffuser ports. Analysis of the outfall's operation over the past two and a half decades, however, demonstrates that it has consistently maintained a high level of effectiveness in effluent dispersal. In fact, without the occasional measurements recorded within the ZID due to vessel drift, the extremely dilute discharge plume might remain undetected within all the vertical profiles collected during a given survey.

It has not always been possible to determine which measurements were subject to permit limits among hydrocasts near the ZID boundary, however. For example, prior to 1999 and before the advent of DGPS, CTD locations could not be determined with sufficient accuracy to establish whether the average station position was located within the ZID, much less how the CTD was moving laterally during the hydrocast. Because of these navigational limitations, sampling was presumed to occur at a single, imprecisely determined, horizontal location. Federal and state reporting of monitoring data still mandates identification of a single position for all of the CTD data collected at a particular station. Thus, for regulatory reporting, and for consistency with past surveys, the May 2017 survey also identifies a single sampling location for each station. These average station positions are identified by the blue stars in Figure 2, and are listed in Table 2 along with their distances from the diffuser structure.

Table 2. Average Position of Vertical Profiles during the May 2017 Survey

	Time (PDT)				Closest Approach	
Station	**Downcast**	**Upcast**	**Latitude**	**Longitude**	**Range[9] (m)**	**Bearing[10] (°T)**
RW1	8:51:07	8:52:21	35° 23.253' N	120° 52.510' W	87.0	4
RW2	8:54:56	8:56:07	35° 23.233' N	120° 52.508' W	50.8	10
RW3	8:58:49	9:00:00	35° 23.212' N	120° 52.507' W	**14.7[11]**	41
RW4	9:02:26	9:03:43	35° 23.189' N	120° 52.502' W	**12.1[12]**	221
RW5	9:05:52	9:07:07	35° 23.164' N	120° 52.502' W	53.9	194
RW6	9:12:01	9:13:09	35° 23.143' N	120° 52.510' W	94.6	195

[7] Below 15.5 m
[8] Refer to the lower left inset in Figure 2.
[9] Distance from the closest open diffuser port to the average profile location
[10] Angle measured clockwise relative to true north from the closest diffuser port to the average profile location
[11] Some of the CTD measurements were located within the ZID boundary (refer to the upper right inset in Figure 2).
[12] Most of the CTD measurements were located within the ZID boundary (refer to lower left inset in Figure 2).

OCEANOGRAPHIC PROCESSES

The trajectory of a satellite-tracked drogued drifter measured oceanic flow throughout the May 2017 survey (Figure 3). Modeled after the curtain-shade design of Davis et al. (1982) and drogued at mid-depth (7 m), a drifter has been deployed during each of the quarterly water column surveys conducted over the past two decades. In this configuration, oceanic flow rather than surface wind dictates the drifter's trajectory, which provides a good indication of the plume's movement after discharge, except when the flow field exhibits strong vertical shear.

During the May 2017 survey, the drifter was deployed near the diffuser structure at 7:12 AM, and was recovered at 9:32 AM at a location 553 m north (356ºT[13]) of its original release point (red dots in Figure 3). The nearly linear drifter track demonstrated that mid-depth oceanic current direction was comparatively consistent throughout the survey. The uniform spacing between the yellow and black dots in Figure 3, which show the drifter's progress at five- and ten-minute intervals, indicates that flow speed varied little from the average speed of 6.6 cm/s.[14] This flow speed was somewhat greater than that observed during most prior surveys. At the rapid transport rate measured during the May 2017 survey, effluent would have experienced only a brief, 3.9-minute residence time within the ZID.

The drifter trajectory accurately captured the transport direction of the effluent plume during the survey, as indicated by the northerly offset observed in the plume signature delineated during the tow surveys.[15] This consistency in directional offset, as well as the absence of a sharply defined thermocline within the water column,[16] suggests that drifter's movement reflected flow throughout most of the water column. If a countercurrent was present, it was restricted to a boundary layer within few meters above the seafloor.

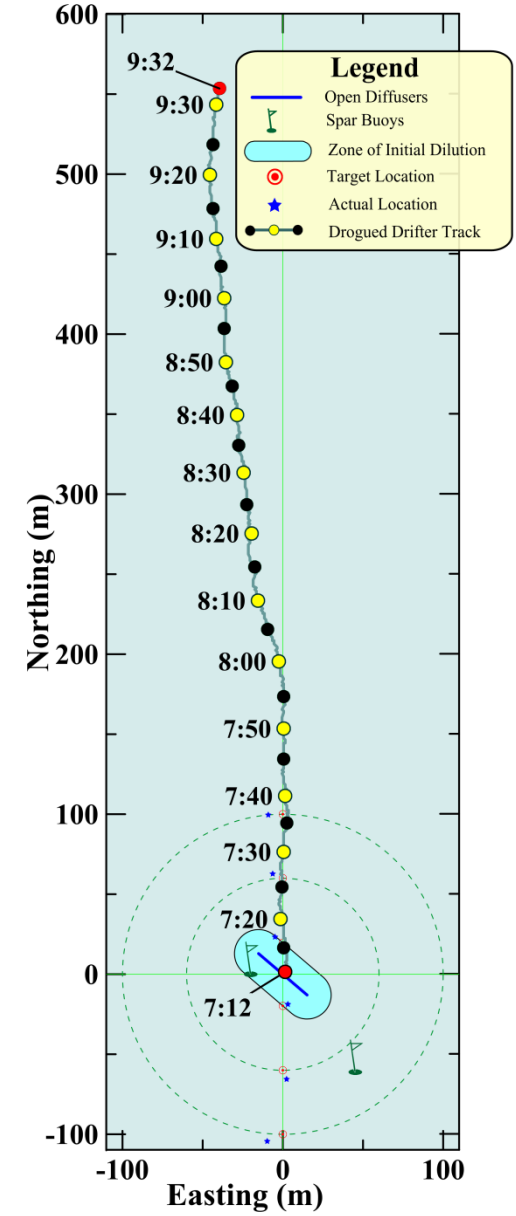

Figure 3. Drogued Drifter Trajectory

[13] Direction measured clockwise relative to true (rather than magnetic) north
[14] 0.127 kt
[15] Refer to Figures 9 and 10 later in this report.
[16] As indicated by the steady vertical change in seawater properties throughout the water column shown in Figure 8 later in this report.

Barotropic (vertically uniform) flow is a hallmark of tidal forcing, and a northward component of flow is consistent with the flood tide that prevailed throughout the survey (Figure 4). However, flow within the survey area is usually influenced by a variety of oceanographic processes in addition to tidal forcing, including upwelling and remote processes, such as large-scale along-shore pressure gradients and the passing of large eddies embedded within the California Current. At any given time, one or more of these processes may control the observed flow field.

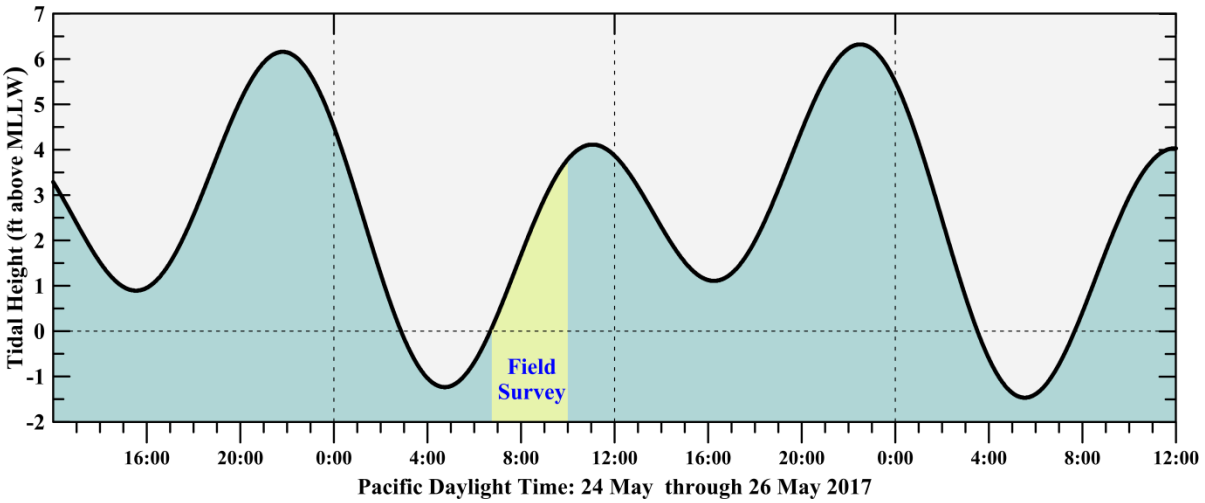

Figure 4. Tidal Level during the May 2017 Survey

Normally along this section of coastline, currents within the survey area are largely determined by the prevailing wind field. Strong and steady northwesterly winds cause upwelling within the water column and produce a system of vertical countercurrents (Figure 5). In the upper water column, net wind-driven Ekman transport occurs at a 90º angle to the prevailing wind.[17] As a result, warm ocean waters within the surface mixed layer are driven offshore (southwestward) in response to the along-shore winds (toward the southeast). Near the coast, these warm surface waters are replaced by deep, cool, nutrient-rich waters that well up from below. The upwelled waters originate farther offshore and move shoreward (northeastward) along the seafloor as part of the upwelling process. Thus, upwelling establishes a vertically sheared current flow within the survey area.

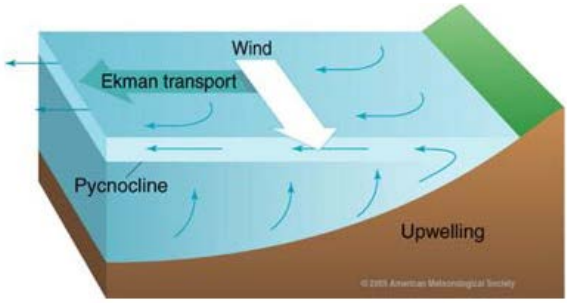

Figure 5. Schematic of Upwelling Processes

The onset of these upwelling-dominated processes normally begins with a rapid intensification of southeastward-directed winds along the central coast during late March and or early April as shown by the positive (blue) upwelling indices in Figure 6. This transition to more persistent southeastward winds is initiated by the stabilization of a high-pressure field over the northeastern Pacific Ocean. Clockwise winds around this pressure field drive prevailing northwesterly winds along the central California coast. The May 2017 survey was conducted during a brief relaxation in upwelling winds that occurred shortly

[17] http://oceanmotion.org/html/background/upwelling-and-downwelling.htm

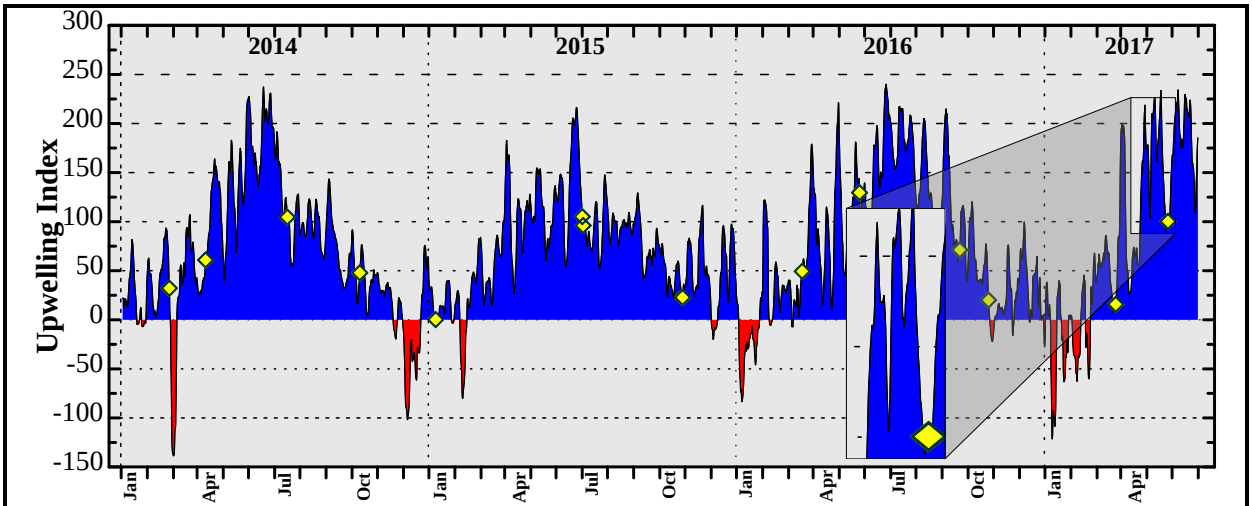

Figure 6. Five-Day Average Upwelling Index ($m^3/s/100$ m of coastline)

after a prolonged month-long period of intense upwelling when indices reached levels more than double the index on the day of the survey (refer to the inset containing the last yellow diamond in Figure 6).

Some degree of upwelling is almost always present during offshore surveys (other yellow diamonds in Figure 6). Throughout most of the year, the nutrient-rich seawater brought to the sea surface near the coast by upwelling enables phytoplanktonic blooms that are the foundation of the productive marine fishery found along the central California coast. The vertical counterflow associated with persistent upwelling conditions also enhances vertical stratification of the water column. The influx of cold dense water at depth produces a thermocline that is commonly maintained throughout summer and into early fall.

During late fall and winter, upwelling is typically weak, and occasionally downwelling events, indicated by the negative (red shaded) indices in Figure 6, occur when passing storms temporarily reverse the normal wind pattern and drive surface waters shoreward. As the surface waters approach the coastline, they downwell, producing nearly uniform seawater properties throughout the water column. An unusual series of severe winter storms at the beginning of 2017 produced multiple downwelling events (refer to the red downward excursions in the upwelling index during January and February 2017 in Figure 6).

Although only moderate upwelling winds were present at the time of the May 2017 survey, winds during the weeks prior to the survey were strong enough to produce a pattern of sea surface temperatures indicative of strong upwelling processes within the central-coast region. This upwelling pattern was captured by the satellite image shown on the cover of this report. The image was recorded by infrared sensors on one of NOAA's polar orbiting satellites during a period of relatively cloudless skies a week prior to the survey. The presence of pools of cooler, upwelled water is visually apparent immediately adjacent to the south-central coastline (dark -blue and magenta shading). The large 4°C difference between these sea-surface temperatures and temperatures farther offshore (in green and yellow) demonstrate that intense upwelling had a profound effect on oceanographic conditions throughout the region.

As upwelling winds began to relax prior to the May 2017 survey, vertical mixing began to erode the sharply defined thermocline normally indicative of an intense upwelling event, leaving behind a gradual vertical gradient in seawater properties. Consequently, the strong northward oceanic flow measured within northern Estero Bay at the time of the survey was probably not solely due to either tidal or upwelling forces. Instead, it is likely that it was driven by other external oceanographic processes, such as

large-scale along-shore pressure gradients, or the passing of an eddy associated with the California Current.

METHODS

The 38 ft F/V *Bonnie Marietta*, owned and operated by Captain Mark Tognazzini of Morro Bay, served as the survey vessel on Friday, 25 May 2017. Douglas Coats of Marine Research Specialists (MRS) supervised scientific operations as Chief Scientist, and provided data-acquisition and navigational support during the survey. He also assisted with the deployment and recovery of the CTD and drifter, and collected meteorological measurements at each station. Crewmember William Skok managed deck operations and collected the Secchi depth measurements at each station.

Auxiliary Measurements

Auxiliary measurements and observations were collected at each of the six stations after completion of the vertical profiling phase of the survey. Standard observations of weather and sea conditions, and beneficial uses, were augmented by visual inspection of the sea surface for floating particulates, oil sheens, and discoloration potentially related to effluent discharge. Other auxiliary measurements collected at each station included wind speeds and air temperatures measured with a handheld Holdpeak 866B Digital Thermo-Anemometer, and oceanic flow measurements made throughout the survey area using the aforementioned drogued drifter.

Additionally, at all six stations, a Secchi disk was lowered through the water column to determine its depth of disappearance. Secchi depths provide a visual measure of near-surface turbidity or water clarity. The depth of disappearance is inversely proportional to the average amount of organic and inorganic material suspended along a line of sight in the upper water column. As such, Secchi depths measure natural light penetration, which can be limited by increased suspended particulate loads from plankton blooms, onshore runoff, seafloor sediment resuspension, and wastewater discharge. They are also biologically meaningful because the depth of the euphotic zone, where most oceanic photosynthesis occurs, is limited to approximately twice the Secchi depth.

Instrumental Measurements

A Sea Bird Electronics SBE-19plusV2 Seacat CTD instrument package collected measurements of conductivity, temperature, light transmittance, dissolved oxygen (DO), pH, and pressure during the May 2017 survey. The six seawater properties used to assess receiving-water quality in this report were derived from the continuously recorded output from the CTD's probes and sensors. Although pressure-housing limitations confine the CTD to depths less than 680 m (Table 3), this is well beyond the maximum depth

Table 3. CTD Specifications

Component	Units	Range	Accuracy	Resolution
Housing (19p-1a; Acetron Plastic)	m	0 to 680	—	—
Pump (SBE 5P)	—	—	—	—
Pressure (19p-2h; Strain-Gauge)	dBar	0 to 680	±1.7	± 0.10
Conductivity	Siemens/m	0 to 9	± 0.0005	± 0.00005
Salinity	‰	0 to 58	± 0.004	± 0.0004
Temperature	ºC	–5 to 35	± 0.005	± 0.0001
Transmissivity (WETLabs C-Star)[18]	%	0 to 100	± 0.3	± 0.03
Oxygen (SBE 43)	% Saturation	0 to 120	± 2	—
pH (SBE 18)	pH	0 to 14	± 0.1	—

[18] 25-cm path length of red (650 nm) light

of the deepest station in the outfall survey. The entire CTD was returned to the factory in January 2015 for full calibration and servicing. The transmissometer and DO probe were returned to the manufacturer in January 2016 for further servicing, repair, and calibration.

The precision and accuracy of the various probes, as reported in manufacturer's specifications, are listed in Table 3. Salinity (‰) was calculated from conductivity measurements reported in units of Siemens/m. Density was derived from contemporaneous temperature (°C) and salinity data, and was expressed as 1000 times the specific gravity minus one, which is a unit of sigma-T (σ_t).

Assessments of all three of the physical parameters (salinity, temperature, and density) helped determine the lateral extent of the effluent plume during the towing phase of the survey. Additionally, during the vertical-profiling phase, they quantified layering, or vertical stratification and stability of the water column, which determines the behavior and dynamics of the effluent as it mixes with seawater within and beyond the ZID. Data on the three remaining seawater properties, light transmittance (water clarity), hydrogen-ion concentration (acidity/alkalinity – pH), and dissolved oxygen (DO), further characterized the receiving waters, and were used to assess compliance with water-quality criteria. Light transmittance was measured as a percentage of the initial intensity of a transmitted beam of light detected at the opposite end of a 0.25-m path. Transmissivity readings are reported relative to 100% transmission in air, so the maximum theoretical transmission in (pure) water is expected to be 91.3%.

Before beginning the mid-depth tow survey at 7:25 AM, the CTD was deployed beneath the sea surface for a seven-minute equilibration period as the vessel was positioned for the first transect. Prior to deployment, the CTD package had been configured for horizontal towing with forward-looking probes. The protective cage around the CTD was fitted with a horizontal stabilizer wing and a depth-suppression weight was added to the towline to achieve near constant-depth tows.

Eight transects of mid-depth data were collected at an average depth of 8.8 m and an average speed of 1.77 m/s over the span of 36 minutes (blue-green lines in Figure 7). Subsequently, at 8:06 AM, eight additional passes were made with the CTD at an average depth of 3.8 m (orange lines). During this 29-minute shallow tow, vessel speed averaged 1.71 m/s.

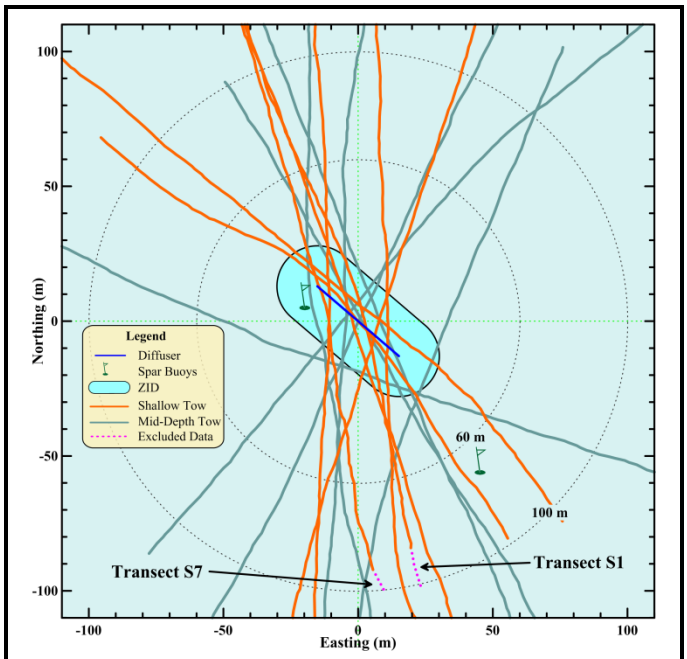

Figure 7. CTD Tracklines during the May 2017 Tow Surveys

At the observed towing speeds and the 4 Hz sampling rate, at least 2.3 CTD measurements were collected for each meter traversed. This complies with the NPDES discharge permit requirement for minimum horizontal resolution of at least one sample per meter during at least five passes around and across the ZID at two separate depths, one within the surface mixed layer and one at mid-depth within the thermocline. Contemporaneous navigation fixes recorded aboard the survey vessel were adjusted for CTD setback and aligned with time stamps on the internally recorded CTD data. The resulting data for the six

seawater properties were then processed to produce horizontal maps within the upper and sub-thermocline portions of the water column.[19]

At 8:35 AM, following completion of the last shallow transect, the CTD package was brought aboard the survey vessel and reconfigured for vertical profiling. The CTD was redeployed at 8:46 AM, and was held beneath the surface for five minutes as the vessel was repositioned over Station RW1. The CTD was then raised to within 0.5 m of the sea surface and profiling commenced. The CTD was lowered at a continuous rate of speed to the seafloor. Measurements at all six stations were collected during a single deployment of the CTD package by towing it below the ocean surface while transiting between adjacent stations.

Quality Control

During the vertical-profiling and horizontal-towing phases of the survey, real-time data were monitored for completeness and range acceptability. Although real-time monitoring indicated that the recorded properties were complete and within acceptable coastal seawater ranges,[20] subsequent post-processing revealed events that impacted portions of the data, resulting in the adjustment or exclusion of these data prior to initiating the compliance analysis. In the case of the May 2016 survey, review of the tow data revealed that the CTD changed depth when the vessel executed a turn at the end of each transect. These vertical offsets in CTD depth are introduced by changes in vessel speed and direction that are instituted to realign the vessel between each transect. Because of the complex interaction between turn radius, vessel speed, and CTD depth, the CTD's target depth cannot always be maintained at these times.

Because the discharge-related anomalies used in the compliance analysis are identified by comparing the amplitudes of measurements acquired at the same depth level, the ability to resolve anomalies with statistical certainty is compromised when data from different depth levels are combined in the horizontal maps. This is particularly true whenever the water column is stratified, as was the case during the May 2017 survey.

However, the exclusion of portions of tow data did not adversely affect the compliance analysis. Only small portions of two transects (S1 and S7) exhibited unacceptable depth offsets within the 100-m survey area (purple dotted lines in Figure 7). The remaining transects were long enough to fully encompass the 100-m survey area surrounding the diffuser structure. Specifically, the tow data that was included in the compliance analysis, shown by the solid orange and blue-green lines in Figure 7, met the permit monitoring requirement of at least five passes near the diffuser structure at each tow depth.

Additionally, the portions of two shallow transects that were excluded because of depth offsets were located on the southern extreme of the survey area, and well outside of the plume footprint. Real-time monitoring of the CTD measurements during the initial portion of the mid-depth tow survey revealed that the plume had been transported well north of the diffuser structure, and in a direction aligned with the drogued drifter movement. In response, covering the southern reaches of the survey area was considered less important than extending the tracklines well to the north.

[19] Figures 9 and 10 later in this report

[20] Field sampling protocols employed during the survey generally followed the field operations manual for the Southern California Bight Study (SCBFMC 2002), which includes CTD cast-acceptability ranges listed in Table 2 of the manual.

RESULTS

The second-quarter receiving-water survey was conducted on the morning of Friday, 25 May 2017. The receiving-water survey commenced at 7:12 AM with the deployment of the drogued drifter. Over the course of the ensuing two hours and twenty minutes, offshore observations and measurements were collected as required by the NPDES monitoring program. The survey ended at 9:33 AM with the retrieval of the drogued drifter. Collection of required visual observations of the sea surface was generally unencumbered throughout the survey.

Auxiliary Observations

On the morning of 25 May 2017, skies were overcast, with a sustained moderate onshore breeze out of the west (Table 4). Auxiliary observations were collected beginning at 9:18 AM, after completion of the vertical profiling phase of the survey. During the subsequent nine minutes, each station was re-occupied beginning with Station RW5, because the vessel happened to be on that station. Next, auxiliary observations were collected at Station RW6, and then stations were re-occupied sequentially progressing toward the north beginning with Station RW4. During that time, wind speed and air temperature remained relatively constant. A swell out of the northwest had a significant wave height of two-to-three feet. At 16°C, average air temperature was somewhat warmer than the 13°C sea surface temperature.

Table 4. Standard Meteorological and Oceanographic Observations

	Location[21]		Diffuser Distance	Time	Air	Cloud Cover	Wind Avg	Wind Dir (from)	Swell Ht/Dir	Secchi Depth
Station	Latitude	Longitude	(m)	(PDT)	(°C)	(%)	(kt)	(°T)	(ft/°T)	(m)
RW1	35° 23.251' N	120° 52.505' W	83.3	9:29:35	14.4	100%	5.6	260	2-3 NW	4.0
RW2	35° 23.233' N	120° 52.501' W	53.7	9:27:56	15.2	100%	4.4	250	2-3 NW	4.0
RW3	35° 23.209' N	120° 52.507' W	10.8	9:25:29	15.9	100%	4.6	290	2-3 NW	4.0
RW4	35° 23.187' N	120° 52.506' W	18.4	9:23:39	16.0	100%	5.2	290	2-3 NW	4.0
RW5	35° 23.168' N	120° 52.507' W	48.8	9:18:32	17.9	100%	4.2	290	2-3 NW	4.0
RW6	35° 23.146' N	120° 52.503' W	84.9	9:21:22	16.4	100%	4.3	260	2-3 NW	4.0

There was no evidence of floating particulates, oil sheens, or any discoloration of the sea surface associated with the presence of wastewater constituents. There was no other visual indication of the presence of the discharge plume at or beneath the sea surface during the survey. Ambient light penetration beneath the sea surface was limited by an increased density of planktonic organisms within the upper water column. During upwelling, nutrients carried upward into the euphotic zone are assimilated by phytoplankton, whose populations increase and, along with their associated zooplanktonic herbivores; their elevated densities reduce the transmittance of ambient light.

Because of the plankton-induced turbidity increase, the Secchi disk faded from view at a relatively shallow depth of 4 m as it was lowered through the upper water column at each station (Table 4). The measured Secchi depth indicates that an 8-m euphotic zone was present during the survey, and that ambient light only penetrated through the upper half of the water column and did not extend to the 8.8-m level where the mid-depth tow was conducted.

Because the Secchi depths were constant among all the stations, near-surface water clarity did not appear to be impacted by the presence of the plume, at least at the locations where the Secchi depth was

[21] Locations are the vessel positions at the time the Secchi depths were measured. These depart from the CTD profile locations listed in Table 2 because they were collected after completion of the CTD profiling.

measured. As discussed below, the rising effluent plume carried slightly more-turbid deep seawater upward to mid-depth, but the plume did not reach the 3.8-m depth where the shallow tow was conducted. Consequently, Secchi depth measurements were not affected by the plume and accordingly, no visual evidence of the plume at or beneath the sea surface was observed at any time during the survey. Similarly, no evidence of floating particulates, oil sheens, or any discoloration of the sea surface was visually apparent that might be related to the presence of wastewater constituents.

Communication with plant personnel and subsequent review of effluent discharge properties on the day of the survey, confirmed that the treatment process was performing well at time of the survey. The 0.866 million gallons of effluent discharged on 25 May had a temperature of 20°C and a pH of 7.4. An effluent sample collected on 24 May, the day prior to the survey, had a suspended-solids concentration of 58 mg/L and a biochemical oxygen demand (BOD) of 51 mg/L. The oil and grease concentration measured within effluent discharged two days prior to the survey was estimated to be 1.6 mg/L, but was too low to be reliably quantified.

Instrumental Observations

Data collected during vertical profiling were processed in accordance with standard procedures (SCCWRP 2002), and are collated at 0.5-m depth intervals in Table 5. Data collected during the May 2017 survey reflect moderately stratified conditions within Estero Bay indicative of a relaxation in coastal upwelling following a month-long pulse of strong upwelling winds that ended five days prior to the May 2017 survey (refer to the inset in Figure 6). As described previously, upwelling of varying intensity occurs most of the year along the central California coast, with the strongest upwelling winds beginning in March or April and extending through the summer. The intensity of upwelling tends to decline into fall, although pulses of sustained northwesterly winds still occur. An intense upwelling event results in the rapid influx of dense, cold, saline water at depth and leads to a sharp thermocline, halocline, and pycnocline where temperature, salinity, and density change rapidly over a small vertical distance. Under these highly stratified conditions, isotherms crowd together to form a density interface that inhibits the vertical exchange of nutrients and other water properties, traps the effluent plume at depth, and reduces the initial dilution of the effluent plume.

If the upwelling winds are only of moderate strength, occur only briefly, or have not occurred recently; vertical mixing slowly erodes the sharp contrast between the surface and deep watermasses, and stratification appears as a more gradual vertical change in seawater properties that can extend throughout the water column. That was the case during the May 2017 survey when seawater properties characteristic of the surface mixed layer steadily changed with increasing depth until they reached ambient seawater conditions more representative of a deep watermass that migrated shoreward along the seafloor during upwelling (Figure 8ef). This gradual vertical transition was interrupted by the rising effluent plume that was captured during hydrocasts at Station RW1, RW2, RW3, and RW4. The steadily changing vertical gradients in ambient seawater properties were altered within the depth ranges where the plume was present, which is delineated by reductions in salinity shown by the green shading in Figure 8abcd.

For the most part, however, the vertical changes in seawater properties within the survey area reflected a gradual transition from shallow conditions established locally by nearshore processes to a colder, saltier, nutrient-rich but oxygen-poor watermass that migrated shoreward along the seafloor as part of the upwelling process. This offshore watermass moved shoreward to replace nearshore surface waters that were driven offshore by Ekman transport from the prevailing northwesterly winds (Figure 5). The seawater properties of this deep watermass originated within the northward-flowing Davidson undercurrent that carried more saline and less oxygenated waters out of the Southern California Bight and northward along the central California coast.

Table 5. Vertical Profile Data Collected on 25 May 2017

Depth (m)	Temperature (°C)						Salinity (‰)					
	RW-1	RW-2	RW-3	RW-4	RW-5	RW-6	RW-1	RW-2	RW-3	RW-4	RW-5	RW-6
0.5	13.101	13.111	12.991	12.925	12.693	12.923	33.800	33.796	33.799	33.795	33.798	33.810
1.0	13.239	13.096	12.763	12.772	12.650	12.789	33.800	33.798	33.793	33.796	33.798	33.802
1.5	13.093	13.041	12.259	12.657	12.582	12.646	33.795	33.797	33.772	33.794	33.797	33.799
2.0	12.888	12.941	11.888	12.525	12.417	12.493	33.792	33.795	33.759	33.790	33.792	33.801
2.5	12.775	12.825	11.746	12.349	12.367	12.327	33.793	33.793	33.777	33.784	33.796	33.796
3.0	12.650	12.715	11.703	12.199	12.229	12.226	33.799	33.791	33.797	33.792	33.796	33.793
3.5	12.379	12.645	11.505	11.969	11.844	12.162	33.790	33.790	33.789	33.790	33.786	33.792
4.0	12.185	12.564	11.123	11.744	11.663	12.066	33.792	33.787	33.739	33.790	33.798	33.790
4.5	11.939	12.463	10.879	11.588	11.582	11.972	33.779	33.788	33.722	33.793	33.803	33.795
5.0	11.660	12.359	10.841	11.540	11.532	11.904	33.752	33.795	33.722	33.799	33.806	33.801
5.5	11.518	11.979	10.834	11.465	11.484	11.782	33.743	33.768	33.728	33.800	33.807	33.806
6.0	11.352	11.539	10.828	11.407	11.354	11.465	33.731	33.753	33.730	33.806	33.807	33.795
6.5	11.059	11.396	10.833	11.366	11.271	11.364	33.703	33.747	33.736	33.810	33.812	33.804
7.0	10.909	11.140	10.832	11.333	11.196	11.331	33.703	33.734	33.736	33.812	33.815	33.807
7.5	10.906	10.904	10.853	11.268	11.127	11.311	33.721	33.730	33.740	33.814	33.817	33.809
8.0	10.952	10.852	10.883	11.213	11.072	11.289	33.751	33.741	33.761	33.815	33.819	33.813
8.5	11.016	10.815	10.881	11.203	11.014	11.213	33.776	33.752	33.777	33.819	33.821	33.815
9.0	11.059	10.735	10.892	11.134	10.981	11.074	33.791	33.753	33.781	33.819	33.823	33.814
9.5	10.954	10.718	10.865	11.076	10.963	10.993	33.767	33.759	33.765	33.821	33.825	33.817
10.0	10.922	10.710	10.841	11.033	10.946	10.969	33.775	33.763	33.763	33.822	33.826	33.821
10.5	10.959	10.701	10.841	11.013	10.930	10.952	33.820	33.769	33.763	33.824	33.826	33.822
11.0	10.850	10.696	10.829	10.922	10.900	10.936	33.820	33.778	33.759	33.824	33.827	33.824
11.5	10.733	10.697	10.729	10.820	10.866	10.902	33.825	33.791	33.762	33.819	33.828	33.824
12.0	10.719	10.708	10.661	10.799	10.859	10.872	33.830	33.807	33.782	33.792	33.829	33.825
12.5	10.648	10.711	10.666	10.795	10.846	10.863	33.832	33.814	33.783	33.787	33.829	33.827
13.0	10.563	10.681	10.662	10.772	10.832	10.856	33.832	33.813	33.786	33.786	33.829	33.828
13.5	10.536	10.623	10.657	10.764	10.821	10.847	33.833	33.817	33.788	33.788	33.831	33.829
14.0	10.529	10.546	10.658	10.682	10.725	10.832	33.834	33.829	33.789	33.787	33.829	33.830
14.5	10.521	10.488	10.634	10.572	10.603	10.778	33.835	33.834	33.796	33.790	33.831	33.829
15.0	10.502	10.472	10.535	10.480	10.517	10.714	33.836	33.836	33.820	33.791	33.834	33.831
15.5	10.464	10.465	10.515	10.469	10.492	10.566	33.837	33.838	33.830	33.818	33.836	33.829
16.0	10.439	10.452	10.486	10.463	10.487	10.505	33.839	33.839	33.835	33.838	33.837	33.833
16.5				10.458	10.493	10.491				33.840	33.847	33.837

Table 5. Vertical Profile Data Collected on 25 May 2017 (continued)

Depth (m)	Density (σ_t)						pH					
	RW-1	RW-2	RW-3	RW-4	RW-5	RW-6	RW-1	RW-2	RW-3	RW-4	RW-5	RW-6
0.5	25.443	25.438	25.464	25.474	25.531	25.507	8.176	8.161	8.151	8.143	8.112	8.126
1.0	25.416	25.442	25.505	25.505	25.531	25.507	8.178	8.168	8.149	8.135	8.113	8.126
1.5	25.441	25.453	25.586	25.527	25.543	25.533	8.178	8.166	8.142	8.126	8.115	8.121
2.0	25.479	25.471	25.647	25.549	25.571	25.564	8.170	8.163	8.119	8.122	8.113	8.115
2.5	25.502	25.493	25.687	25.579	25.584	25.591	8.161	8.156	8.096	8.115	8.113	8.109
3.0	25.531	25.513	25.711	25.613	25.611	25.609	8.161	8.150	8.080	8.110	8.113	8.110
3.5	25.577	25.525	25.741	25.655	25.676	25.620	8.165	8.142	8.069	8.106	8.091	8.109
4.0	25.616	25.539	25.772	25.697	25.719	25.637	8.153	8.141	8.049	8.092	8.065	8.106
4.5	25.653	25.559	25.802	25.729	25.737	25.659	8.137	8.141	8.000	8.064	8.052	8.100
5.0	25.684	25.585	25.808	25.742	25.749	25.676	8.097	8.140	7.958	8.044	8.040	8.091
5.5	25.703	25.636	25.814	25.757	25.759	25.703	8.059	8.141	7.934	8.032	8.033	8.090
6.0	25.724	25.707	25.817	25.772	25.783	25.753	8.036	8.117	7.924	8.022	8.025	8.073
6.5	25.755	25.729	25.821	25.783	25.802	25.778	7.993	8.074	7.918	8.017	8.023	8.053
7.0	25.782	25.765	25.821	25.790	25.817	25.787	7.957	8.038	7.913	8.015	8.023	8.038
7.5	25.797	25.804	25.820	25.804	25.832	25.792	7.936	7.991	7.909	8.014	8.018	8.034
8.0	25.812	25.822	25.831	25.815	25.843	25.799	7.926	7.946	7.910	8.008	8.015	8.030
8.5	25.819	25.836	25.844	25.819	25.855	25.815	7.932	7.926	7.914	8.007	8.009	8.030
9.0	25.824	25.852	25.846	25.832	25.862	25.839	7.952	7.917	7.915	8.008	8.003	8.026
9.5	25.824	25.859	25.838	25.844	25.867	25.855	7.945	7.899	7.913	8.008	8.000	8.020
10.0	25.835	25.864	25.841	25.852	25.871	25.863	7.933	7.889	7.908	8.003	7.995	8.014
10.5	25.864	25.870	25.841	25.857	25.874	25.867	7.927	7.883	7.903	8.001	7.990	8.008
11.0	25.883	25.878	25.839	25.873	25.880	25.871	7.924	7.878	7.902	7.994	7.987	8.003
11.5	25.908	25.888	25.859	25.888	25.887	25.877	7.907	7.872	7.899	7.984	7.981	7.999
12.0	25.914	25.898	25.887	25.871	25.889	25.883	7.896	7.873	7.884	7.969	7.974	7.991
12.5	25.929	25.903	25.887	25.868	25.891	25.886	7.891	7.871	7.873	7.959	7.969	7.983
13.0	25.943	25.908	25.890	25.871	25.894	25.889	7.886	7.873	7.870	7.951	7.963	7.976
13.5	25.949	25.921	25.893	25.874	25.897	25.891	7.878	7.872	7.868	7.945	7.953	7.974
14.0	25.951	25.944	25.893	25.887	25.913	25.894	7.873	7.869	7.865	7.929	7.937	7.966
14.5	25.953	25.958	25.903	25.909	25.935	25.903	7.870	7.852	7.861	7.912	7.902	7.950
15.0	25.957	25.962	25.939	25.926	25.953	25.916	7.867	7.839	7.850	7.881	7.867	7.934
15.5	25.965	25.965	25.950	25.949	25.959	25.940	7.860	7.831	7.835	7.859	7.848	7.905
16.0	25.970	25.968	25.959	25.965	25.961	25.954	7.843	7.826	7.826	7.850	7.836	7.882
16.5				25.968	25.961	25.959				7.828	7.827	7.852

Table 5. Vertical Profile Data Collected on 25 May 2017 (continued)

Depth (m)	Dissolved Oxygen (mg/L)						Transmissivity (%)					
	RW-1	RW-2	RW-3	RW-4	RW-5	RW-6	RW-1	RW-2	RW-3	RW-4	RW-5	RW-6
0.5	9.467	9.340	8.976	8.809	8.658	8.701	77.924	78.969	79.099	78.599	78.118	78.403
1.0	9.214	9.103	8.427	8.693	8.730	8.557	79.070	79.018	78.297	78.144	77.866	77.847
1.5	9.207	8.945	8.307	8.724	8.831	8.589	78.914	78.968	78.104	77.206	77.276	77.496
2.0	9.382	8.912	8.513	8.871	8.842	8.844	78.586	78.790	78.754	76.969	77.971	77.500
2.5	9.471	8.998	8.397	8.860	8.533	8.898	78.254	78.550	78.927	78.470	78.298	77.644
3.0	9.338	9.123	7.736	8.450	8.183	8.796	78.709	78.220	79.180	79.220	78.365	77.953
3.5	9.130	9.254	6.761	8.043	8.220	8.740	79.436	78.034	80.573	79.860	79.091	78.682
4.0	8.470	9.355	6.591	7.954	8.136	8.714	80.005	78.135	80.591	79.667	79.250	78.923
4.5	8.006	9.030	6.584	7.854	8.028	8.639	80.009	78.358	79.190	80.080	79.552	79.137
5.0	7.771	8.143	6.572	7.732	7.931	8.182	79.573	78.627	78.392	80.358	80.242	78.852
5.5	7.299	7.723	6.566	7.800	8.034	7.947	78.791	78.659	78.080	80.251	80.590	79.229
6.0	6.702	7.526	6.562	7.852	8.082	8.049	78.727	79.079	77.999	81.010	80.572	79.904
6.5	6.590	6.912	6.578	7.832	8.024	8.086	78.469	79.070	78.141	81.632	80.678	80.827
7.0	6.676	6.608	6.626	7.784	7.998	8.083	77.373	78.673	78.084	81.562	81.115	80.632
7.5	6.892	6.568	6.674	7.787	7.946	8.101	77.217	78.531	78.101	82.222	81.268	80.840
8.0	7.164	6.396	6.692	7.814	7.840	7.993	77.444	77.978	78.085	81.839	81.247	80.909
8.5	7.040	6.188	6.651	7.851	7.802	7.857	78.062	78.003	78.272	81.653	80.810	81.162
9.0	6.678	6.149	6.562	7.808	7.759	7.824	79.325	77.896	78.788	81.241	80.993	81.186
9.5	6.745	6.083	6.555	7.702	7.703	7.831	79.026	77.686	78.776	81.980	81.883	81.597
10.0	6.739	6.055	6.556	7.619	7.635	7.823	78.378	77.217	78.630	81.578	81.976	81.874
10.5	6.379	6.068	6.414	7.320	7.513	7.747	79.030	77.221	78.624	81.630	81.436	82.260
11.0	6.312	6.093	6.078	7.106	7.414	7.559	79.729	77.079	78.199	81.846	81.343	82.234
11.5	6.316	6.120	6.028	7.081	7.373	7.447	79.435	76.768	78.030	81.865	80.903	82.043
12.0	6.226	6.111	6.038	6.975	7.174	7.394	79.612	77.057	77.176	82.350	81.052	82.402
12.5	6.055	6.061	6.022	6.796	7.111	7.281	80.338	77.459	76.939	82.352	81.500	82.231
13.0	6.028	5.931	5.998	6.687	6.927	7.135	80.689	78.319	77.006	82.471	81.542	82.316
13.5	6.018	5.727	5.989	6.142	6.054	6.881	79.663	78.563	77.095	82.378	81.875	82.582
14.0	5.976	5.552	5.756	5.601	5.804	6.615	79.802	78.633	77.049	81.865	82.087	82.439
14.5	5.841	5.547	5.600	5.466	5.577	6.165	79.324	77.904	77.105	79.822	81.609	82.121
15.0	5.513	5.519	5.574	5.468	5.515	5.645	79.407	76.363	76.501	76.170	78.617	82.094
15.5	5.489	5.526	5.505	5.444	5.485	5.535	78.206	75.730	76.281	74.731	74.772	80.274
16.0	5.886	5.608	5.558	5.403	5.467	5.572	78.388	74.782	75.110	74.119	74.276	78.803
16.5				5.451	5.445	5.685				74.319	74.395	77.612

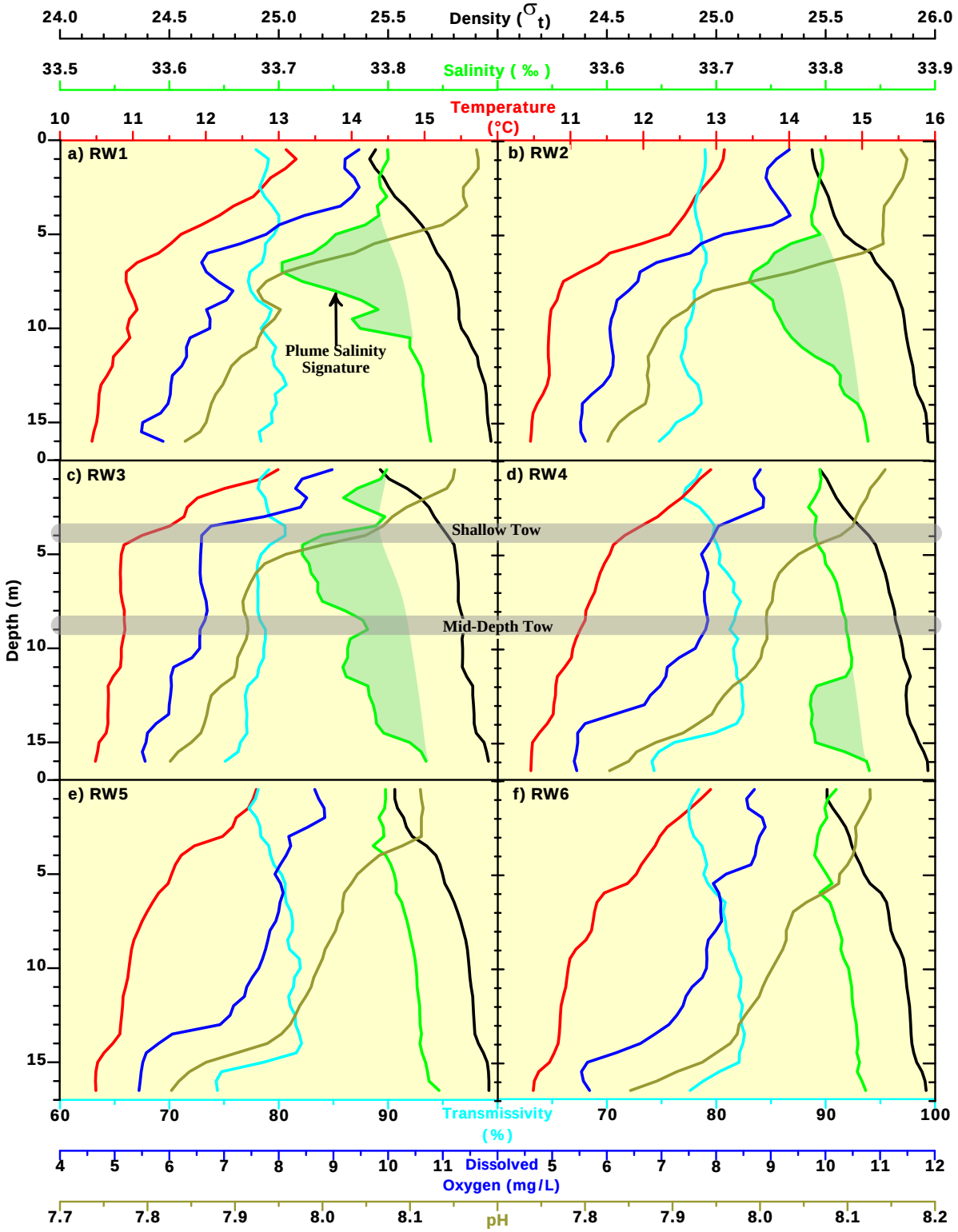

Figure 8. Vertical Profiles of Water-Quality Parameters

Thus, upwelling in the weeks prior to the survey produced predicable changes in seawater properties within this vertical transition zone between the shallow and deep watermasses; namely, seawater properties exhibited steadily increasing or decreasing values with depth that were determined by well-established physicochemical processes (Figure 8ef). Specifically, temperature (red lines), DO (dark blue lines), pH (olive-colored lines) steadily decreased with increasing depth. These decreases were mirrored by a halocline and pycnocline, where salinity (green lines) and density (black lines) steadily increased with depth. Transmissivity (light blue lines) also steadily increased with increasing depth until the 2.5-m-thick seafloor boundary layer associated with the deep watermass was encountered.

Within the shallow reaches of the water column, upwelling-enhanced primary productivity produced oxygen (increasing DO), consumed carbon dioxide (increasing pH), and slightly decreased water clarity (light blue lines) due to the increased phytoplankton density. In contrast, the lower temperature, DO, and pH, and increased salinity of the seafloor watermass resulted from its origin deep offshore. Because it had not been in recent direct contact with the atmosphere, biotic respiration and decomposition had depleted its DO levels (dark blue lines). Additionally, at depth, biotic respiration and decomposition produced carbon dioxide (CO_2), and in its dissolved state, the increased concentration of carbonic acid appears as a concomitant reduction in pH (olive-colored lines).

As expected from its increased density, the deep watermass migrated shoreward along the seafloor, which accounts for the sharper reductions in temperature, DO, and pH seen within the seafloor layer below 14 m (red, dark-blue, and gold lines in Figure 8ef). Additionally, this 2.5-m thick seafloor layer was significantly more turbid than the overlying layer as reflected by a sharp reduction in transmissivity (light blue lines). This vertical contrast generated a local transmissivity maximum near 14 m in many of the vertical profiles. The 8% decline in seafloor transmissivity within the deep watermass arose because of naturally occurring resuspension processes associated with boundary layer flow along the seafloor. During upwelling, the shoreward transport of offshore waters along the seafloor occasionally generates increased turbulence and shear within a benthic nepheloid layer (BNL). These thin, transient, particle-rich layers form when lightweight flocs of detritus are resuspended by the turbulence generated from bottom currents. BNLs are a widespread phenomenon on continental shelves (Kuehl et al. 1996) and have been regularly documented in past surveys conducted within Estero Bay.

In addition to the aforementioned influence of natural processes on the vertical trends in seawater properties, the downcasts at Stations RW1 through RW4 (Figure 8abcd) encountered the effluent plume at various depth levels as the plume rose within the water column and was transported northward. Its presence perceptibly altered the vertical distribution of ambient seawater properties. Not surprisingly, the most pronounced plume effect was apparent in the profiles at Station RW3 (Figure 8c), which was located immediately downstream (down current) of the diffuser structure. At that ZID station, the largest salinity declines spanned a remarkably wide depth range from 4 m to 15 m (green shading on the salinity profile). Within that depth range, other seawater properties were nearly vertically uniform compared to the steadily changing properties in ambient seawater (*cf*, the red, dark-blue, gold, and light-blue lines in Figure 8c with 8e).

The vertical uniformity in seawater properties at Station RW3 resulted from the upward transport of the ambient seawater found at depth within the deep watermass. Near the seafloor, this cold turbid seawater mixed rapidly with effluent shortly after discharge, and the diluted effluent took on the surrounding ambient seawater properties, which were then carried upward in the water column by buoyant effluent plume. As the plume approached the sea surface, it compressed the gradual vertical gradients seen at Stations unaffected by the plume (Southern Stations RW5 and RW6 in Figure 8ef), into a very sharp vertical transition zone above 4 m (red, dark-blue, and gold lines in Figure 8c). As the plume migrated farther north to Stations RW1 and RW2, the plume's vertical extent began to collapse around its equilibrium (trapping) depth near 7 m as it began to spread laterally (light green shading in Figures 8ab).

The presence of a deep plume signature at the up-current Station RW4 (light green shading between 12 m and 15.5 m in Figure 8d) indicates that the flow direction within the BNL was opposite (southward) of the northward flow measured within the rest of the water column. Thus, because of the vertically sheared flow, the plume initially migrated toward the south shortly after discharge when it was within the BNL. As the plume began to ascend above the BNL boundary, the strong prevailing northward current carried it rapidly in the opposite direction and toward the three stations on the northern side of the diffuser structure.

The vertical profile data also demonstrate that vertical stratification within the water column at the time of the survey was of sufficient strength to trap the effluent plume beneath the sea surface. During most surveys, when the water column is less stratified, the buoyant plume rises all the way to the sea surface where it spreads laterally. On those occasions, the location of surfacing plume is often visually apparent as a reduction in capillary waves over a limited area within the ZID. However, during stratified conditions, the plume can become trapped at depth, which curtails the additional buoyant mixing normally experienced during the plume's ascent through the entire water column.

Although the vertical profile data at Stations RW1 and RW2 demonstrate that the subsurface plume had become trapped at a depth near 7 m (light green shading in the salinity profiles of Figure 8ab), the May 2017 survey data also provide unusual insight into the dynamics of the plume trapping process. Specifically, the smaller isolated salinity reduction above 3 m at Station RW3 (Figure 8c) demonstrates that the momentum of the rising effluent plume initially carried it well beyond its buoyant-equilibrium depth and close to the sea surface. Subsequently, the positive buoyancy of the dilute effluent-seawater mixture caused the plume to descend as it was transported farther north by the prevailing current. These vertical oscillations about the buoyancy equilibrium depth are a well-described phenomenon in atmospheric and oceanographic dynamics. In fact, the buoyancy oscillation frequency can be determined analytically from the strength of water-column stratification.[22]

The northward migration of the rising effluent plume that was revealed in the vertical hydrocasts was also captured by the tow surveys (Figures 9 and 10). The mid-depth tow was conducted at a depth (8.8 m) that was slightly beneath the 7 m plume trapping depth (thick shaded line spanning Figure 8cd). Nevertheless, the mid-depth tow captured the lower portion of the plume during its northward migration beyond the ZID (Figure 9abdef). In contrast, the 3.8-m shallow tow was conducted well above the trapping depth. As a result, the shallow tow only captured the plume signature within a limited area of the ZID (Figure 10abcef) where its upward momentum briefly caused it to overshoot its buoyancy equilibrium level. Its positive buoyancy at that location was confirmed by plume density measurements that were higher than the surrounding seawater (note the reversed density scale in Figure 10c). In contrast, the near-neutral plume density close to the trapping depth was reflected by the absence of density anomalies associated with the plume signature during the mid-depth tow (Figure 9c).

Additionally, in Figure 10d, the absence of a shallow plume transmissivity signature arose because reduced-transmissivity BNL seawater entrained within the plume was comparable to that of the ambient seawater near the sea surface (both were approximately 78% in the light blue line of Figure 8f). Thus, there was little contrast between plume transmissivity and that of the surrounding ambient seawater in the upper water column. On the contrary, water clarity was naturally higher at mid-depth, so the BNL seawater within the plume exhibited a distinct contrast in the mid-depth transmissivity map (Figure 9d).

[22] The Väisälä-Brunt frequency, or buoyancy frequency, is the frequency at which a vertically displaced water parcel will oscillate within a statically stable environment. Because of its direct relation to stability, it is often cited as an alternative measure of the degree of water-column stratification.

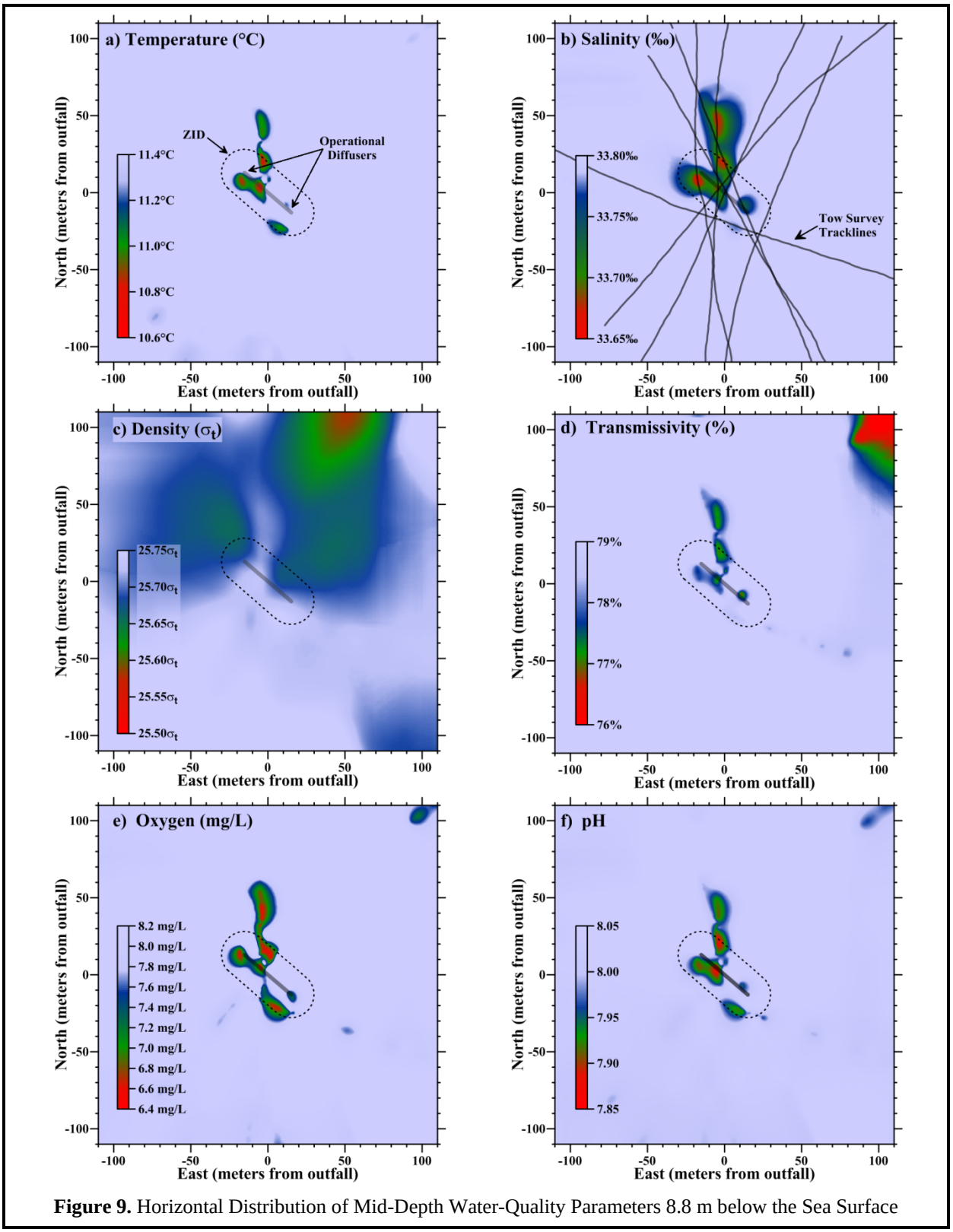

Figure 9. Horizontal Distribution of Mid-Depth Water-Quality Parameters 8.8 m below the Sea Surface

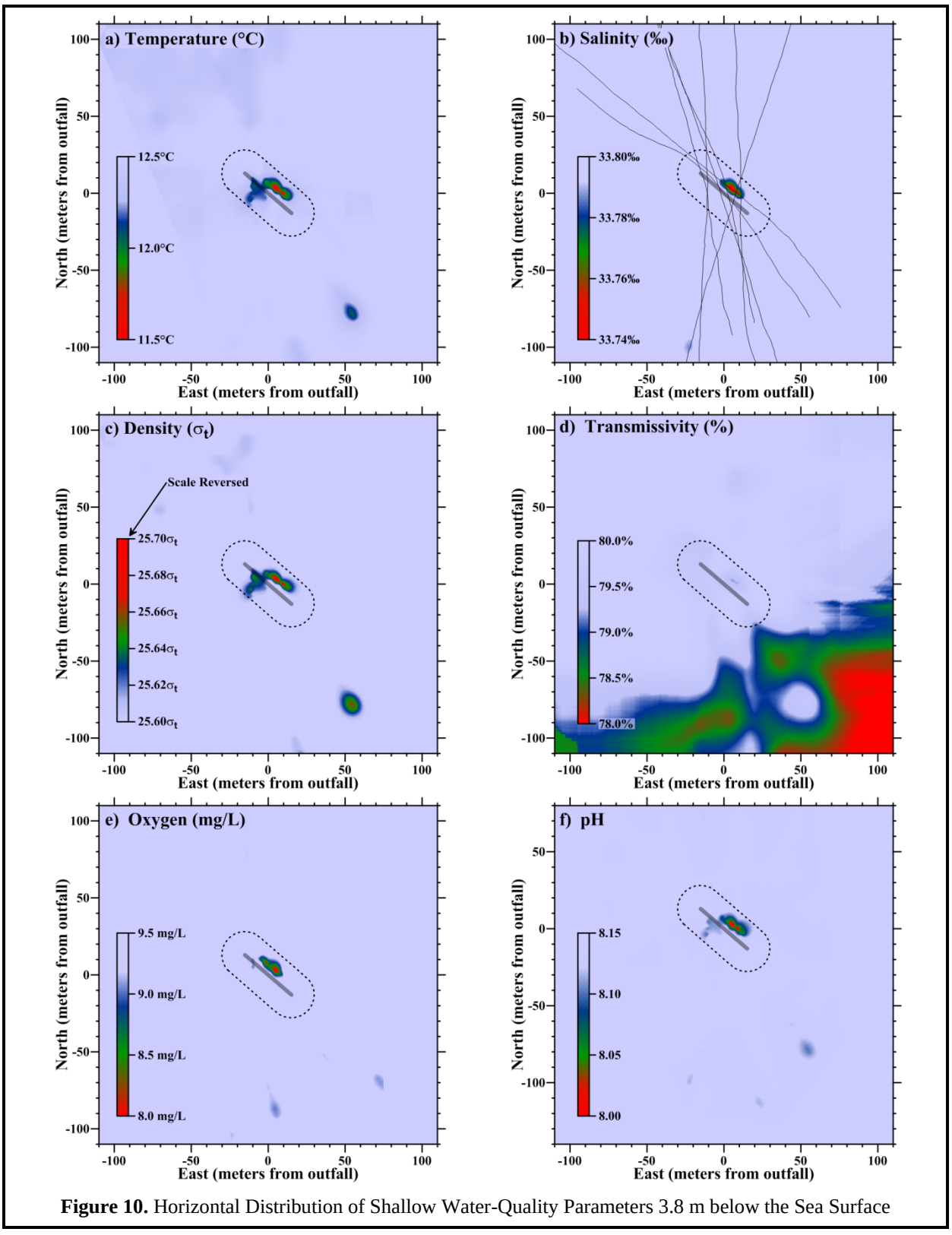

Figure 10. Horizontal Distribution of Shallow Water-Quality Parameters 3.8 m below the Sea Surface

Thus, the plume-related excursions seen in temperature, transmissivity, DO, and pH during the survey were largely caused by the entrainment and upward transport of ambient seawater. It is important to distinguish plume signatures that are caused by the presence of effluent constituents, exemplified by marked reductions in salinity, from those caused by the upward transport of ambient seawater, embodied by the lateral anomalies in all the other seawater properties. Close to the seafloor, intense mixing is driven by the momentum of the effluent's ejection from the individual diffuser ports. Subsequent turbulent mixing caused by the plume's ascent through the water column is less intense, and as a result, the dilute effluent plume tends to retain the ambient seawater properties it acquired at the seafloor. During the May 2017 survey, these deep seawater properties became apparent as a signature of the buoyant effluent plume when they were juxtaposed against the ambient seawater characteristics in the mid and upper water column. These entrainment-generated anomalies are only apparent, however, when the water column is sufficiently stratified to cause a perceptible contrast between the shallow and deep ambient seawater properties.

The legacies of entrainment anomalies can be particularly long-lived, remaining apparent within the water column well after completion of the initial dilution process. As such, these anomalies provide useful tracers of the diffuse effluent plume during and after the completion of the initial dilution process. However, such anomalies are irrelevant to the receiving-water compliance assessment because the permit restricts attention to water-quality changes caused solely by the presence of wastewater constituents rather than by a simple relocation of ambient seawater.

Outfall Performance

The current efficacy of the outfall can be evaluated through a comparison of dilution levels measured at the time of the May 2017 survey, and dilutions anticipated from modeling studies that were codified in the discharge permit through limits imposed on effluent constituents. Specifically, the critical initial dilution applicable to the MBCSD outfall was conservatively estimated to be 133:1 (Tetra Tech 1992). That is, dispersion modeling estimated that, at the conclusion of the minimum expected initial mixing, 133 parts of ambient seawater would have mixed with each part of wastewater.

The 133:1 dilution estimate was based on worst-case modeling under highly stratified conditions, where trapping of the plume below a strong thermocline would curtail the additional buoyant mixing normally experienced during the plume's ascent through the entire water column. Additionally, the modeling assumed quiescent oceanic flow conditions, thereby restricting initial mixing processes to the ZID. Under those conditions, the modeling predicted that a 133:1 dilution would be achieved after the plume rose only 9 m from the seafloor, whereupon it would become trapped, ceasing to ascend further in the water column. At that point, the plume would spread laterally with dilution occurring at a much-reduced rate. A 9-m ascent at the MBCSD outfall translates into a trapping depth that is 6.4 m below the sea surface. As described below, however, the dilution levels observed during the May 2017 survey were much higher than the 133:1 predicted by the modeling, even though they were measured within the ZID and well before the completion of the initial dilution process.

The conservative nature of the critical initial dilution determined from the modeling is an important consideration because it was used to specify permit limitations on chemical concentrations within wastewater discharged from the treatment plant. These end-of-pipe effluent limitations were back calculated from the receiving-water objectives in the COP (SWRCB 2005) using the projected 133-fold dilution determined from the modeling. Application of a higher critical dilution would relax the stringent end-of-pipe effluent limitations thought necessary to meet COP objectives after initial dilution is complete.

End-of-pipe limitations on contaminant concentrations within discharged wastewater were based on the definition of dilution (Fischer et al. 1979). From the mass-balance of a conservative tracer, the concentration of a particular chemical constituent within effluent before discharge (C_e) can be determined from Equation 1.

$$C_e \equiv C_o + D\left(C_o - C_s\right) \qquad \text{Equation 1}$$

where: C_e = the concentration of a constituent in the effluent,
C_o = the concentration of the constituent in the ocean after dilution by D (i.e., the COP receiving-water objective),
D = the dilution expressed as the volumetric ratio of seawater mixed with effluent, and
C_s = the background concentration of the constituent in ambient seawater.

By rearranging Equation 1, the actual dilution achieved by the outfall can be determined from measured seawater anomalies. This measured dilution can then be compared with the critical dilution factor determined from modeling. Salinity is an especially useful tracer because it directly reflects the magnitude of ongoing dilution. The regions of slightly lower salinity apparent north of the outfall in both tow-survey maps (Figures 9b and 10b), and in the vertical profiles measured at most stations (Figure 8abcd) were induced by the presence of dilute wastewater. These salinity anomalies document mixing-processes within the effluent plume shortly after discharge, and as it rose through the water column and spread laterally near its trapping depth.

The amplitudes of these salinity anomalies quantify the magnitude of wastewater dilution at the various stages of the initial mixing process. By rearranging Equation 1, the dilution ratio (D) can be computed from the salinity anomaly ($A = C_o - C_s$) as:

$$D \equiv \frac{(C_e - C_o)}{\left(C_o - C_s\right)} \propto A^{-1} \qquad \text{Equation 2}$$

The salinity concentration within MBCSD effluent (C_e)[23] is small compared to that of the receiving seawater and, after dilution by more than 133-fold, the salinity of the effluent-seawater mixture is close to ambient salinity. Consequently, to a close approximation, dilution levels are inversely proportional to the amplitude of the salinity anomaly. Thus, a lower effluent dilution at a given location within the effluent plume is directly mirrored by a larger reduction in the measured salinity relative to that of the surrounding seawater.

Among the 11,393 CTD measurements collected during the May 2017 survey, the greatest reduction in salinity (-0.166‰) was recorded during the fifth transect of the mid-depth tow survey when a salinity of 33.643‰ was encountered only 3 m from the middle of the diffuser structure at a depth of 8.9 m (red shading in Figure 9b). From Equation 2, this salinity anomaly corresponds to a dilution of 196-fold (small patch of red close to the center of the diffuser structure in Figure 11).

[23] Wastewater samples have an average salinity of 0.995‰.

However, the mid-depth tow also encountered other pools of low salinity that were located as much as 50 m farther north. These low salinity pools corresponded to increasingly higher dilutions with increasing distance from the diffuser. The northernmost pool contained effluent that had been diluted at least 220-fold (northernmost patch of red shading in Figure 11). The increased dilution within the northern patches arose from enhanced mixing associated with vertical buoyancy oscillations around the trapping depth that were described previously. The mid-depth pool encounters appear as patches in the horizontal maps because the plume moved laterally as it oscillated vertically, and thus, porpoised in and out of the mid-depth tow level.

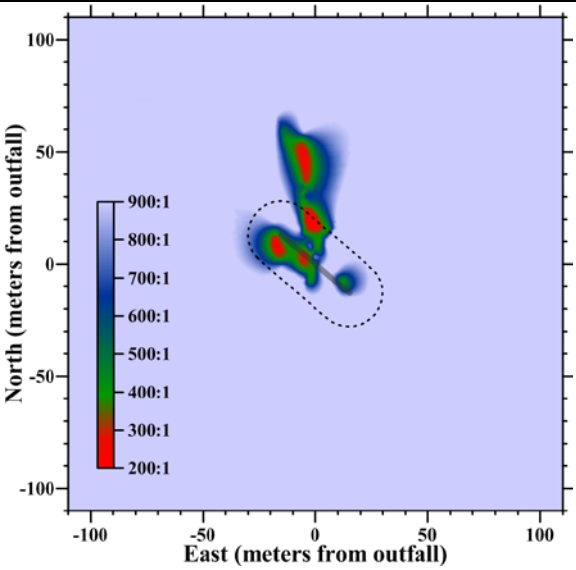

Figure 11. Mid-Depth Plume Dilution Computed from Salinity Anomalies in Figure 9b

Thus, the mid-depth tow data indicate that the plume was continuing to experience rapid initial dilution well beyond the ZID because of buoyancy oscillations around the 7-m trapping depth. By the time the plume reached Station RW1, 100 m north the diffuser structure, the damped vertical oscillations had largely dissipated and the plume had settled near its equilibrium level (Figure 8a). The -0.108‰ salinity reduction at that point corresponds to a 300-fold dilution.

As described previously, the upward momentum of the plume initially carried it close to the sea surface where its upper portions were captured by the shallow tow (Figure 10abcef). However, the associated salinity reductions were weak and highly localized (Figure 12). Although dilution levels were measured down to 354-fold within a few individual salinity measurements, the overall lateral extent of perceptible plume constituents, namely, with dilution levels below 500:1, was limited to an area only 8.5 m in length.

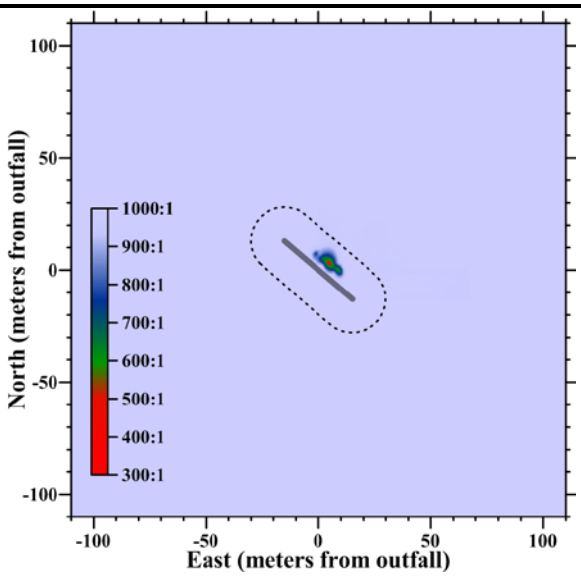

Figure 12. Shallow Plume Dilution Computed from Salinity Anomalies in Figure 10b

Overall, the dilution computations show that, during the May 2017 survey, the outfall was performing better than designed and was rapidly entraining seawater shortly after discharge. This resulted in dilution levels exceeding 196-fold only 3 m from the diffuser structure and long before the initial mixing process was complete. Although this dilution level was measured 2.5 m deeper than the trapping depth assumed in the worst-case modeling study, the plume had already achieved dilution levels 50% higher than predicted. As the plume was transported rapidly to the north, vertical buoyancy-inducted oscillations further increased the dilution to 220-fold before achieving a dilution of 300-fold dilution at the completion of the initial mixing process. At that point, effluent dilution was more than double the 133:1 critical initial dilution used to establish end-of-pipe permit limitations on contaminant concentrations within wastewater discharged from the MBCSD

treatment plant. This demonstrates that, during the May 2017 survey, the COP receiving-water objectives were being easily met by the limits on chemical concentrations within discharged wastewater that are promulgated by the NPDES discharge permit issued to the MBCSD.

COMPLIANCE

This section evaluates compliance with the water-quality limitations listed in the NPDES permit (Table 6). The limits themselves are based on criteria in the COP, the Central Coast Basin Plan, and other state and federal policies that were designed to protect marine life and beneficial uses of ocean waters. Because the limits only pertain to changes in water properties that are caused by the presence of wastewater constituents beyond the ZID, instrumental measurements undergo a series of screening procedures prior to numeric comparison with the permit thresholds. Specifically, the quantitative analyses described in this section focus on water-property excursions caused by the presence of wastewater constituents beyond the ZID, whose amplitudes can be reliably discerned against the backdrop of ambient fluctuations. A detailed understanding of ambient seawater properties, and their natural variability within the region surrounding the outfall, is therefore an integral part of the compliance evaluation presented in this section.

Table 6. Permit Provisions Addressed by the Offshore Receiving-Water Surveys

Limit #	Limit
P1	Floating particles or oil and grease to be visible on the ocean surface
P2	Aesthetically undesirable discoloration of the ocean surface
P3	Temperature of the receiving water to adversely affect beneficial uses
P4	Significant reduction in the transmittance of natural light at any point outside the ZID
P5	The DO concentration outside the zone of initial dilution to fall below 5.0 mg/L or to be depressed more than 10% from that which occurs naturally
P6	The pH outside the zone of initial dilution to be depressed below 7.0, raised above 8.3, or changed more than 0.2 units from that which occurs naturally

The results of the analyses performed on the May 2017 data demonstrate that the MBCSD discharge complied with the NPDES discharge permit. Moreover, although observations within the ZID are not subject to compliance evaluations, they met the prescribed limits because actual dilution levels routinely exceeded the conservative design specifications assumed in the discharge permit. Thus, the quantitative evaluation described in this section documents an outfall and treatment process that was performing at a high level during the May 2017 survey.

Permit Provisions

The offshore receiving-water surveys are designed to assess compliance with objectives dealing with undesirable alterations to six physical and chemical characteristics of seawater. Specifically, the permit states that wastewater constituents within the discharge shall not cause the limits listed in Table 6 to be exceeded.

The first two receiving-water limits, P1 and P2, rely on qualitative visual observations for compliance evaluation. Compliance was demonstrated during the May 2017 survey through visual inspection of the sea surface that documented an absence of floating wastewater materials, oil, grease, and discoloration of the sea surface.

Compliance with the remaining four receiving-water limitations is quantitatively evaluated through a comparison between instrumental measurements and numerical limits listed in the NPDES permit. For

example, in P5 and P6, the fixed numeric limits on absolute values of DO (>5 mg/L) and pH (7.0 to 8.3) can be directly compared with field measurements within the dilute wastewater plume beyond the ZID. However, both P5 and P6 also contain narrative limits, which originate within the COP, and define unacceptable water-quality impacts in terms of "*significant*" excursions beyond those that occur "*naturally*." Quantitative evaluation of these limits requires a further comparison of field measurements with numerical thresholds that reflect the natural variation in temperature, transmissivity, DO, and pH within the receiving waters surrounding the outfall.

As described in prior sections, natural variation in seawater properties can result from a variety of oceanographic processes. These processes establish the range in ambient seawater properties caused by natural spatial variation within the survey region at a given time (e.g., vertical stratification), and by temporal variations caused by seasonal and interannual influences (e.g., El Niño and La Niña). Of particular interest are upwelling and downwelling processes that not only determine average properties at a given time, but also the degree of water-column stratification, or spatial variability, present during any given survey.

Screening of Measurements

Evaluating whether any of the 11,393 CTD measurements collected during the May 2017 survey exceeded a permit limit can be a complex process. For example, although apparently significant excursions in an individual seawater property may be related to the presence of wastewater constituents, they may also result from instrumental errors, natural processes, entrainment of ambient bottom water in the rising effluent plume, statistical uncertainty, ongoing initial mixing within and beyond the ZID, or other anthropogenic influences (e.g., dredging discharges or oil spills).

Because of this complexity, measurements were first screened to determine whether numerical limits on individual seawater properties even apply (Table 7). The screening procedure sequentially applies three questions to restrict attention to: 1) the oceanic area where permit provisions pertain; 2) changes due to the presence of wastewater particulates; and 3) changes large enough to be reliably detected against the backdrop of natural variation. The measurements that remain after completing the screening process can then be compared with Basin-Plan numerical limits and COP allowances.

Table 7. Receiving-Water Measurements Screened for Compliance Evaluation

Topic Addressed	Screening Question	Answer		
		No	**Yes**[24]	***Parameter***
Location	1. Was the measurement collected beyond the 15.2-m ZID boundary where modeling assumes that initial dilution is complete?	*1,628*	*9,765*	All
Wastewater Constituents	2. Did the beyond-ZID measurement coincide with a quantifiable salinity anomaly (≤550:1 dilution level) indicating the presence of detectable wastewater constituents?	*9,501*	*264*	All
Natural Variation	3. Did seawater properties associated with the wastewater measurements depart significantly from the expected range in ambient seawater properties at the time of the survey?	*264*	*0*	Temperature
		264	*0*	Transmissivity
		264	*0*	DO
		264	*0*	pH

[24] Number of remaining CTD observations of potential compliance interest based on sequential application of each successive screening question

The subsection following this one provides additional lines-of-evidence that demonstrate compliance with numerical permit limits independent of the screening process. The rationale for identifying observations suitable for further compliance analysis is presented in the following descriptions of the three screening steps.

1. Measurement Location: The COP states that compliance with its receiving-water objectives "*shall be determined from samples collected at stations representative of the area within the waste field where initial dilution is completed.*" Initial dilution includes the mixing that occurs from the turbulence associated with both the ejection jet, and the buoyant plume's subsequent ascent through the water column.

Although currents often transport the plume well beyond the ZID before the initial dilution process is complete, the COP states that dilution estimates shall be based on "*the assumption that no currents, of sufficient strength to influence the initial dilution process, flow across the discharge structure.*" Because of this, the regulatory mixing distance, which is equal to the 15.2-m water depth of the discharge, provides a conservative boundary to screen receiving-water data for subsequent compliance evaluation. Application of this initial screening question to the May 2017 dataset eliminated 1,628 of the original 11,393 receiving-water observations from further consideration because they were collected within the ZID (Table 7, Question 1). The remaining 9,765 observations were carried forward in the screening analysis.

2. Presence of Wastewater Constituents: The MBCSD discharge permit restricts application of the numerical receiving-water limits to excursions caused by the presence of wastewater constituents. This confines the compliance analysis to changes caused "*as the result of the discharge of waste,*" as specified in the COP, rather than anomalies that arise from the upward movement of ambient seawater entrained within the buoyant effluent plume. Analyses conducted on quarterly receiving-water surveys over the last decade have demonstrated that the direct influence of dilute wastewater is almost never observed in any seawater property other than salinity, except very close (<1 m) to a diffuser port and within its ejection jet.

In fact, negative salinity anomalies are the only consistent indicator of the presence of wastewater constituents within receiving waters. Wastewater salinity is negligible compared to that of the receiving seawater, so the presence of a distinct salinity minimum provides *de facto* evidence of the presence of wastewater constituents. Because of the large contrast between the nearly fresh wastewater and the salty receiving water, salinity provides a powerful tracer of dilute wastewater that is unrivaled by other seawater properties. Other properties do not exhibit such a large contrast and, as such, their wastewater signatures dissipate rapidly upon discharge with very little mixing. Wastewater's lack of salinity, however, provides a definitive tracer that allows the presence of effluent constituents to be identified even after dilution many times greater than the 133-fold critical initial dilution assumed in the discharge permit.

As described in the previous section, wastewater-induced reductions in salinity can be used to determine the amount of dilution achieved by initial mixing. Based on statistical analyses of the natural variability in salinity readings measured near the outfall over a five-year period between 2004 and 2008, the smallest reduction in salinity that can be reliability detected within receiving waters is 0.062‰. This represents a dilution level of 542-fold in Equation 2. Salinity reductions that are smaller than 0.062‰ cannot be reliably discerned against the backdrop of natural variation, and would not result in discernible changes in other seawater properties. Eliminating those measurements from further evaluation restricts attention to excursions in temperature, light transmittance, DO, and pH that are potentially related to the presence of wastewater constituents.

As discussed previously, the greatest salinity reductions observed during the May 2017 survey were recorded immediately north of the outfall during the mid-depth tow survey. Because of the strong oceanic flow, the submerged plume was carried well beyond the ZID as it experienced vertical buoyancy-induced oscillations before the initial dilution process was complete. As a result, an unusually large number of quantifiable salinity reductions were measured well north of the ZID boundary. Even though these 264 salinity anomalies were clearly measured prior to completion of the initial dilution process, they were outside the ZID and reliably associated with the presence of wastewater constituents (Table 7). The remaining 9,501 salinity measurements collected beyond the ZID during the May 2017 survey did not have salinity reductions that were larger than the 0.062‰ plume-detection threshold, and therefore corresponded to dilutions greater than 550:1.

3. Natural Variation: An integral part of the compliance analysis is determining whether a particular anomalous measurement resulted from the presence of wastewater constituents, or whether it simply became apparent because ambient seawater was relocated (upward) by the plume. If the measurement does not significantly depart from the natural range in ambient seawater properties at the time of the survey, then it is inappropriate to ascribe the departure to the presence of wastewater constituents. Thus, quantifying the natural variability around the outfall at the time of the survey is necessary for determining whether a particular observation warrants comparison with the numeric permit limits.

A statistical analysis of receiving-water data collected around the outfall was used to establish the range in natural conditions surrounding the outfall (first three data columns of Table 8 on the following page). These ambient-variability ranges were used to identify significant departures from natural conditions that could be indicative of adverse discharge-related effects on water quality. The same five-year database used to establish the within-survey salinity variation discussed previously, was also used to establish one-sided 95% confidence bounds on transmissivity (-10.2%), temperature (+0.82°C), DO (-1.38 mg/L), and pH (± 0.094). These were combined with 95th percentiles determined from the May 2017 ambient seawater data, to establish time-specific natural-variability thresholds in a manner analogous to COP Appendix VI. The percentiles were determined from May-2017 vertical profile data collected largely at Stations RW5 and RW6, and excluded all measurements potentially affected by the discharge at other stations.

Temperature, transmissivity, pH, and DO concentrations associated with the 264 remaining measurements of potential compliance interest were all well within their respective ranges of natural variability (Table 7, Question 3). As such, the screening process unequivocally eliminated all of the measurements collected during the May 2017 survey from further consideration in the compliance analysis. In fact, all of the documented excursions in these properties were the result of physical processes unrelated to the presence of wastewater constituents, namely, entrainment of near-bottom seawater within the rising effluent plume.

As described previously, anomalies in seawater properties clearly delineated the plume, but those entrainment-generated excursions were not caused by the presence of wastewater constituents. During periods when the water column is even slightly stratified, ambient seawater properties near the seafloor differ from those within the rest of the water column, and their juxtaposition within the rising effluent plume appears as lateral anomalies within the upper water column. Regardless, if the presence of wastewater particulates had contributed to the observed decreases in DO, pH and transmissivity within the upper water column, their influence would still have been well within the natural range of the ambient seawater properties at the time of the survey. Consequently, their influence on water quality would not be considered environmentally significant.

Table 8. Compliance Thresholds

Water Quality Property	95% Confidence Bound[25]	95th Percentile[26,27]	Natural Variability Threshold[28]	COP Allowance[29]	Basin Plan Limit[30]	Extremum[31]
Temperature (ºC)	0.82	12.93	>13.75	>15.94	—	≤13.24
Transmissivity (%)	-10.2	75.1	<64.9	—	—	≥73.3
DO (mg/L)	-1.38	5.49	<4.11	<3.69	<5.00	≥5.40
pH (minimum)	-0.094	7.838	<7.743	<7.543	<7.000	≥7.826
pH (maximum)	0.094	8.164	>8.258	>8.548	>8.300	≤8.206

Other Lines of Evidence

Several additional lines of evidence further support the conclusion that all the CTD measurements collected during the May 2017 survey complied with the quantitative permit limits P3 through P6 in Table 6. In combination, these lines of evidence provide the "best explanation" of the origin and significance of individual measurements using abductive inference (Suter 2007). This process, which has been used to implement sediment-quality guidelines for California estuaries (SWRCB 2009), emphasizes a pattern of reasoning that accounts for both discrepancies and concurrences among multiple lines of evidence. A best explanation approach serves to limit the uncertainty associated with each individual CTD measurement, and to provide a more robust compliance assessment. Together, these lines of evidence significantly strengthen the conclusion that the discharge fully complied with the permit at the time of the May 2017 survey.

Natural Variability within and beyond the ZID: Although the permit limits only apply to changes in DO, pH, temperature, and transmissivity beyond the ZID, examination of measurements acquired within the ZID frequently provides additional insight into the potential for adverse effects on water quality. However, among all the data collected during the May 2017 survey, salinity was the only seawater property that exhibited a perceptible difference from ambient conditions. Regardless of their association with the plume's effluent salinity signature or their proximity to the diffuser structure, none of the 11,393 temperature, DO, pH, and transmissivity observations exceeded the thresholds of natural variability

[25] The one-sided confidence bound measures the ability to reliably determine ambient seawater properties within surveys as a whole. They were determined from an analysis of the variability in ambient water-quality data collected during 20 quarterly surveys conducted between 2004 and 2008. Although water-quality observations potentially affected by the presence of wastewater constituents were excluded from the analysis, more than 9,200 remaining observations for each of the six seawater properties accurately quantified the inherent uncertainty in defining the range in natural conditions.

[26] The COP (Appendix I, Page 27, SWRCB 2005) defines a "*significant*" difference as "*a statistically significant difference in the means of two distributions of sampling results at the 95% confidence level.*" Accordingly, COP effluent analyses (Step 9 in Appendix VI, Page 42, Ibid.) are based "*the one-sided, upper 95% confidence bound for the 95th percentile.*"

[27] The 95th-percentile quantified natural variability in seawater properties during the May 2017 survey itself, and was determined from vertical-profiles data unaffected by the discharge.

[28] Thresholds represent limits on wastewater-induced changes to receiving-water properties that significantly exceed natural conditions as specified in the discharge permit and COP. They are determined from the sum of columns to the left and are specific to the May 2017 survey. They do not include the COP allowances specified in the column to the right.

[29] The discharge permit, in accordance with the COP, allows excursions in seawater properties that depart from natural conditions by specified amounts. DO cannot be "*depressed more than 10% from that which occurs naturally,*" and pH cannot be "*changed more than 0.2 units from that which occurs naturally.*" The California Thermal Plan is incorporated into the COP by reference, and restricts temperature increases to less than 2.2ºC.

[30] Permit limits P5 and P6 (Table 6) include specific numerical values promulgated in the RWQCB Basin Plan (1994) in addition to changes relative to natural conditions specified in the COP. The Basin Plan upper-bound pH objective for ocean waters is 8.5, but a more-stringent upper-bound objective of 8.3, which applies to individual beneficial uses, was implemented in the MBCSD discharge permit.

[31] Maximum or minimum value measured during the May 2017 survey, regardless of location within or beyond the ZID

specified in Table 8. This is apparent from a comparison between the extrema listed in the last data column in Table 8, and the corresponding natural-variability thresholds listed in third data column. For example, ambient seawater temperatures are expected to range as high as 13.75ºC, but the highest measured temperature was 13.24ºC. Similarly, natural excursions in transmissivity are expected to range as low as 64.9%, while the lowest measured transmissivity was 73.3%.

COP Allowances: The COP does not explicitly require that wastewater-induced changes remain within the ranges in natural variation listed in the third data column of Table 8, even though these ranges were conservatively used in the data screening process described in previous subsections. Consideration of these COP allowances for receiving-water limits provides an additional safety factor in the compliance evaluation of thermal, DO, and pH excursions.

For pH, the COP and the discharge permit allow changes up to 0.2 pH units from natural conditions, bringing the minimum allowed pH down to 7.543 for the May 2017 survey (fourth data column of Table 8). This limiting value is significantly less than the lowest pH measurement of 7.826 recorded during the May 2017 survey.[32] Similarly, the lowest DO concentration measured during the survey (5.40 mg/L) was well above the lower bound in expected natural variability (4.11 mg/L) and even more so for the less-stringent 10% compliance threshold promulgated by the COP (3.69 mg/L).

Limited Ambient Light Penetration: Although there are no explicit numerical objectives for discharge-related reductions in transmissivity, a numerical limit can be established from the COP requirement that the discharge not result in significant reductions in the transmission of natural light (P4 in Table 6). Because the COP does not specify an allowance beyond natural conditions, the 64.9% threshold on ambient transmissivity variations listed in third data column of Table 8 can be interpreted to constitute a numerical limit.

However, the COP objective for light penetration only applies to a portion of the transmissivity measurements. Because little natural light is present beneath the euphotic zone, which extends to approximately twice the Secchi depth, the limit on transmissivity reductions during the May 2017 survey only applies to measurements recorded above 8 m (twice the average Secchi depth listed in Table 4). This immediately eliminates about half of the transmissivity measurements from further compliance consideration, even though they were included in the screening analysis. Specifically, even if the discharge of wastewater particulates had caused transmissivity measurements collected below the euphotic zone to drop below the numeric compliance threshold, it would not have been of regulatory concern because the penetration of ambient light would not have been affected. This includes measurements collected shortly after discharge near a diffuser port, or those within the naturally turbid BNL above the seafloor, because virtually no natural light was present near the seafloor during the May 2017 survey.

Insignificant Thermal Impact: As with transmissivity, there are no explicit numerical objectives for discharge-related increases in temperature. Nevertheless, a numerical limit can be established for thermal excursions that is based on the requirement that they not adversely affect beneficial uses (P3 in Table 6). Although the COP remains silent regarding allowable temperature changes, it incorporates the California Thermal Plan requirements by reference (COP Introduction §C.3). The Thermal Plan (SWRCB 1972) restricts temperature increases caused by new discharges to coastal water to be less than 2.2°C (4°F). As with DO and pH, a quantitative permit limit on temperature increases can be established by combining the Thermal Plan allowance with the natural variability threshold listed in the third data column of Table 8. Accordingly, increases in temperature caused by the discharge of warm wastewater during the May 2017

[32] Compliance with COP maximum pH allowance (8.349) is irrelevant because effluent on the day of the survey had a pH of 7.4, which is much lower than the lowest pH measured within the receiving seawater (7.826). Consequently, the presence of effluent constituents could not have induced an increase in pH within receiving waters.

survey could be deemed to adversely affect beneficial uses if they exceeded 15.94°C (fourth data column of Table 8). However, none of the 11,393 CTD measurements collected during the survey exceeded 13.24°C (last column in Table 8). As a result, all the measurements remained well within the natural variability thermal threshold (13.75°C), and provided a much larger safety factor for compliance with the numerical limit derived from the Thermal Plan. In reality, temperatures measured within the rising effluent plume were uniformly below that of the surrounding seawater because cooler seawater near the seafloor had been entrained in the plume shortly after discharge. Consequently, any potential thermal impact resulting from the discharge of warm wastewater was almost immediately eliminated upon discharge because the effluent entrained much colder seawater near the seafloor.

Directional Offset: Analysis of the directional offset of CTD measurements is useful because wastewater and receiving-seawater properties depart from one another in several predictable ways. Specifically, upon discharge, wastewater is fresher, warmer, more turbid, and less dense than the ambient receiving waters of Estero Bay. As such, the presence of wastewater constituents will reduce the salinity, density, and transmissivity of the receiving seawater (negative offset), while temperature will be increased (positive offset). Therefore, the reduced temperatures observed in conjunction with the effluent plume during the tow surveys (Figures 9a and 10a) could not have been generated by the presence of warmer wastewater constituents. Instead, they were produced because the plume entrained cooler bottom water shortly after discharge. The observed directional offset was opposite of receiving-water impacts expected from the presence of wastewater constituents.

Insignificant Wastewater Particulate Loads: Another independent line of evidence demonstrates that the discharge of wastewater particulates could not have contributed materially to turbidity within the dilute effluent plume, even before completion of the initial mixing process. The suspended-solids concentration measured onshore, within the effluent, and immediately prior to discharge from the WWTP on 24 May 2017 was 58 mg/L. After dilution by at least 196-fold, the effluent suspended-solids concentration would have the reduced ambient transmissivity by no more than 1.9%. This small potential decrease in transmissivity is overwhelmed by the large 8% decrease in ambient transmissivity caused by the resuspension of seafloor sediments within the BNL.

Similarly, the MBCSD discharge could not have contributed materially to the observed DO fluctuations. The MBCSD treatment process routinely removes 80% or more of the organic material, as demonstrated by the 51-mg/L BOD measured within the plant's effluent on the day prior to the survey. That small amount of BOD would have induced a DO depression of no more than 0.022 mg/L after dilution (MRS 2002). In fact, in the absence of a tangible BOD influence, wastewater discharge would actually be expected to increase DO within subsurface receiving waters, rather than decrease it. This is because effluent is oxygenated by recent contact with the atmosphere during the treatment process, whereas receiving waters at depth are typically depleted in DO due to the long absence of atmospheric equilibration within the deep offshore watermass.

Excursions remained within the fixed Basin-Plan Limits: Permit provisions P5 and P6 (Table 6) combine receiving-water objectives from both the COP and the Basin Plan with regard to DO and pH limits. As described previously, the COP requires that DO concentrations outside the ZID not be depressed more than 10% from that which occurs naturally, and restricts pH measurements to those within 0.2 units of that which occurs naturally. In contrast, the Basin-Plan's fixed numerical limits do not provide specific guidance as to how they might change in response to widespread changes in oceanographic conditions unrelated to the discharge. Specifically, the fixed numerical limits restrict DO concentrations outside the ZID to no less than 5 mg/L (P5 in Table 6), and pH levels to the 7.0-to-8.3 range (P6). As such, the fixed Basin-Plan limit on DO is significantly more restrictive than the 3.69 mg/L minimum allowable DO concentration established for the May 2017 survey under COP objectives. Nevertheless, all of the DO measurements complied also with the more conservative Basin-Plan limit on

DO reductions. In contrast, the minimum allowable pH (7.0) specified in the Basin Plan was less restrictive than the COP limit (7.534) specified for the May 2017 Survey, so all the pH observations again complied with both regulations.

CONCLUSIONS

The quantitative screening analysis demonstrated that all measurements recorded during the May 2017 survey complied with the receiving-water limitations specified in the NPDES discharge permit. This conclusion was further strengthened by other lines of evidence supporting compliance with the discharge permit. Specifically, although discharge-related changes in seawater properties were observed during the May 2017 survey, the changes were either not of significant magnitude (i.e., they were within the natural range of variability that prevailed at the time of the survey), were measured within the boundary of the ZID where initial mixing is still expected to occur, or were not directly caused by the presence of wastewater constituents within the water column (i.e., were entrainment generated).

Early in the initial mixing process, effluent was being diluted to levels in excess of 196-fold, which is markedly higher than the critical dilution levels predicted by design modeling after completion of the mixing process. Later in the initial mixing process, the plume's depth oscillated vertically about its buoyancy equilibrium level as it was rapidly transported to the north. During these buoyancy oscillations, dilution levels reached 220-fold. At the completion of the initial mixing process, effluent had been diluted 300 times. All of the measured dilution levels far exceed levels that were predicted by modeling and that were incorporated in the discharge permit as limits on contaminant concentrations within effluent prior to discharge. Lastly, all of the auxiliary observations collected during the May 2017 survey demonstrated that the discharge complied with the narrative receiving-water limits in the discharge permit and the COP. Together; these observations demonstrate that the treatment process, diffuser structure, and the outfall continue to surpass design expectations.

REFERENCES

Davis, R.E., J.E. Dufour, G.J. Parks, and M.R. Perkins. 1982. Two Inexpensive Current-Following Drifters. Scripps Institution of Oceanography, University of California, San Diego, La Jolla, California. SIO Reference No. 82-28. December 1982.

Fischer, H.B., E.J. List, R.C.Y. Koh, J. Imberger, and N.H. Brooks. 1979. Mixing in Inland and Coastal Waters. New York: Academic Press, 482 p.

Kuehl, S.A., C.A. Nittrouer, M.A. Allison, L. Ercilio, C. Faria, D.A. Dukat, J.M. Jaeger, T.D. Pacioni, A.G. Figueiredo, and E.C. Underkoffler 1996. Sediment deposition, accumulation, and seabed dynamics in an energetic fine-grained coastal environment. *Continental Shelf Research*, 16: 787-816.

Marine Research Specialists (MRS). 1998. City of Morro Bay and Cayucos Sanitary District, Offshore Monitoring and Reporting Program, Semiannual Benthic Sampling Report, April 1998 Survey. Prepared for the City of Morro Bay, CA. July 1998.

Marine Research Specialists (MRS). 2002. City of Morro Bay and Cayucos Sanitary District, Supplement to the 2002 Renewal Application For Ocean Discharge Under NPDES Permit No. Prepared for the City of Morro Bay and Cayucos Sanitary District, Morro Bay, CA. July 2002.

Marine Research Specialists (MRS). 2011. City of Morro Bay and Cayucos Sanitary District, Offshore Monitoring and Reporting Program, 2010 Annual Report. Prepared for the City of Morro Bay, California. March 2011.

Marine Research Specialists (MRS). 2012. City of Morro Bay and Cayucos Sanitary District, Offshore Monitoring and Reporting Program, 2011 Annual Report. Prepared for the City of Morro Bay, California. March 2012.

Marine Research Specialists (MRS). 2013. City of Morro Bay and Cayucos Sanitary District, Offshore Monitoring and Reporting Program, 2012 Annual Report. Prepared for the City of Morro Bay, California. March 2013.

Marine Research Specialists (MRS). 2014. City of Morro Bay and Cayucos Sanitary District, Offshore Monitoring and Reporting Program, 2013 Annual Report. Prepared for the City of Morro Bay, California. March 2014.

National Academy of Sciences. 1993. Managing Wastewater in Coastal Urban Areas. National Research Council Committee on Wastewater Management for Coastal Urban Areas, Water Science and Technology Board, Commission on Engineering and Technical Systems. 477 pp.

Regional Water Quality Control Board (RWQCB) - Central Coast Region. 1994. Water Quality Control Plan (Basin Plan) Central Coast Region. Available from the RWQCB at 81 Higuera Street, Suite 200, San Luis Obispo, California. 148p. + Appendices.

Regional Water Quality Control Board (RWQCB) - Central Coast Region and the Environmental Protection Agency (USEPA) – Region IX. 1992a. Waste Discharge Requirements (Order No. 92-67) and Authorization to Discharge under the National Pollutant Discharge Elimination System (Permit No. CA0047881) for City of Morro Bay and Cayucos Sanitary District, San Luis Obispo County.

Regional Water Quality Control Board (RWQCB) - Central Coast Region and the Environmental Protection Agency (USEPA) – Region IX. 1992b. Monitoring and Reporting Program No. 92-67 for City of Morro Bay and Cayucos Sanitary District, San Luis Obispo County (Permit No. CA0047881).

Regional Water Quality Control Board (RWQCB) - Central Coast Region and the Environmental Protection Agency (USEPA) – Region IX. 1998a. Waste Discharge Requirements (Order No. 98-15) and National Pollutant Discharge Elimination System (Permit No. CA0047881) for City of Morro Bay and Cayucos Sanitary District, San Luis Obispo County. 11 December 1998.

Regional Water Quality Control Board (RWQCB) - Central Coast Region and the Environmental Protection Agency (USEPA) – Region IX. 1998b. Monitoring and Reporting Program No. 98-15 for City of Morro Bay and Cayucos Sanitary District, San Luis Obispo County. 11 December 1998.

Regional Water Quality Control Board (RWQCB) - Central Coast Region and the Environmental Protection Agency (EPA) – Region IX. 2009. Waste Discharge Requirements (Order No. R2-2008-0065) and National Pollutant Discharge Elimination System (Permit No. CA0047881) for the Morro Bay and Cayucos Wastewater Treatment Plant Discharges to the Pacific Ocean, Morro Bay, San Luis Obispo County. Effective 1 March 2009.

Sea-Bird Electronics, Inc. (SBE) 1989. Calculation of M and B Coefficients for the Sea-Tech Transmissometer. Application Note No. 7, Revised September 1989.

Sea-Bird Electronics, Inc. (SBE) 1992. SBE 12/22/22/20 Dissolved Oxygen Sensor Calibration and Deployment. Application Note No. 12-1, rev B, Revised April 1992.

Southern California Bight Field Methods Committee (SCBFMC). 2002. Field Operation Manual for Marine Water-Column, Benthic, and Trawl monitoring in Southern California. Technical Report 259. Southern California Coastal Water Research Project. Westminster, CA. March 2002.

State Water Resources Control Board (SWRCB). 1972. Water Quality Control Plan for Control of Temperature in the Coastal and Interstate Waters and Enclosed Bays and Estuaries of California. Revises and supersedes the policy adopted by the State Board on January 7, 1971, and revised October 13, 1971, and June 5, 1972. California Division of Water Quality, Water Quality Planning Unit.

State Water Resources Control Board (SWRCB). 2005. Water Quality Control Plan, Ocean Waters of California, California Ocean Plan. California Environmental Protection Agency. Effective February 14, 2006.

State Water Resources Control Board (SWRCB). 2009. Water Quality Control Plan for Enclosed Bays and Estuaries – Part 1 Sediment Quality. California Environmental Protection Agency. Effective August 22, 2009. sed_qlty_part1.pdf [Accessed 02/26/10].

Suter II, Glenn, W. 2007. Ecological risk assessment, 2nd edition. U. S. Environmental Protection Agency, Cincinnati, Ohio. CRC.

Tetra Tech. 1992. Technical Review City of Morro Bay, CA Section 201(h) Application for Modification of Secondary Treatment Requirements for a Discharge into Marine Waters. Prepared for the U.S. Environmental Protection Agency, Region IX, San Francisco, CA by Tetra Tech, Inc., Lafayette, CA. February 1992.